Three-dimensional conflict count models for unstructured and layered airspace designs

Sunil, Emmanuel; Ellerbroek, Joost; Hoekstra, Jacco M.; Maas, Jerom

DOI
10.1016/j.trc.2018.05.031

Publication date
2018

Document Version
Accepted author manuscript

Published in
Transportation Research Part C: Emerging Technologies

Three-Dimensional Conflict Count Models for Unstructured and Layered Airspace Designs

Emmanuel Sunil[a,*], Joost Ellerbroek[a], Jacco M. Hoekstra[a], and Jerom Maas[a]

[a] *Faculty of Aerospace Engineering, Delft University of Technology, Kluyverweg 1, 2629 HS, Delft, The Netherlands*

Abstract

This paper presents analytical models that describe the safety of unstructured and layered en route airspace designs. Here, 'unstructured airspace' refers to airspace designs that offer operators complete freedom in path planning, whereas 'layered airspace' refers to airspace concepts that utilize heading-altitude rules to vertically separate cruising aircraft based on their travel directions. With a focus on the *intrinsic* safety provided by an airspace design, the models compute instantaneous conflict counts as a function of traffic demand and airspace design parameters, such as traffic separation requirements and the permitted heading range per flight level. While previous studies have focused primarily on conflicts between cruising aircraft, the models presented here also take into account conflicts involving climbing and descending traffic. Fast-time simulation experiments used to validate the modeling approach indicate that the models estimate instantaneous conflict counts with high accuracy for both airspace designs. The simulation results also show that climbing and descending traffic caused the majority of conflicts for layered airspaces with a narrow heading range per flight level, highlighting the importance of including all aircraft flight phases for a comprehensive safety analysis. Because such trends could be accurately predicted by the three-dimensional models derived here, these analytical models can be used as tools for airspace design applications as they provide a detailed understanding of the relationships between the parameters that influence the safety of unstructured and layered airspace designs.

Keywords: airspace safety, airspace design, conflict probability, conflict rate, Air Traffic Management (ATM)

*Corresponding author
Email address: e.sunil@tudleft.nl (Emmanuel Sunil)

Nomenclature

Greek Letters

α	Heading range per flight level [^{o}]
β	No. of flight levels in 1 layer set
γ	Flight path angle [^{o}]
κ	Number of layer sets
ψ	Aircraft heading [^{o}]
ρ	Density [ac/NM^2]
ε	Proportion of cruising aircraft
ζ	Vertical spacing between layers [ft]

Roman Letters

A	Airspace area [NM^2]
B	Airspace volume [NM^2·ft]
C	No. of instantaneous conflicts
D	Trip Distance [NM]
k	Model accuracy parameter
L	Total No. of flight levels
N	No. of instantaneous aircraft
p	Average conflict probability between any two aircraft
S_h	Horizontal separation requirement [NM]
S_v	Vertical separation requirement [ft]
t_l	Conflict look-ahead time [mins]
V	Aircraft velocity [kts]
V_r	Relative velocity [kts]
Z	Altitude [ft]

Subscripts

$_h$	Horizontal
$_i$	Aircraft i
$_j$	Flight level j
$_v$	Vertical
$_{2d}$	Two dimensional
$_{3d}$	Three dimensional
$_{cd}$	Climbing/Descending aircraft
$_{cruise}$	Cruising aircraft
$_{lay}$	Layered airspace
$_{max}$	Maximum
$_{min}$	Minimum
$_{total}$	Total
$_{ua}$	Unstructured Airspace

1. Introduction

The sustained growth of air traffic in recent years has stressed several components of the current Air Traffic Management (ATM) system to near saturation levels. This is particularly true for en route airspace design where continued reliance on the fixed airway network has significantly reduced flight efficiencies [1]. This is because airway navigation often force aircraft to deviate from direct trajectories, which during peak demand periods can trigger artificial traffic concentrations and increased delays [2, 3]. Their use in Europe, for instance, has been linked to the 20% increase in en route delays in 2016, even though traffic demand grew by only 2.4% during the same time period [4]. Similar statistics reported in many other parts of the world have motivated several studies to explore alternate options for organizing en route traffic [5, 6, 7].

To overcome the capacity limitations posed by airway routing, some researchers have proposed a transition to less rigid route structures for en route airspace [8, 9, 10, 11, 12]. This approach has been adopted in some low-density areas of Europe with the creation of so called 'Free Route Airspaces' (FRAs) since 2008 [13]. FRAs aim to emulate the route selection flexibility offered to aircraft flying in unmanaged airspace, while continuing to provide air traffic controllers with control of the traffic within them. Analysis by Eurocontrol has shown that the limited use of FRAs thus far has yielded an average route efficiency increase of 1.6% per flight, with gains of up to 4% in some areas [4]. Further extending FRAs into more dense airspace sectors could, therefore, lead to substantial reductions in total delay,

fuel consumption and emissions. As such, FRAs demonstrate the potential of utilizing procedural mechanisms to reorganize and improve the performance of en route airspace operations, without large capital investments in new hardware.

While reducing structural constraints can increase en route airspace capacity relative to airway routing for current traffic demand levels, a recent study has found that offering operators *complete* freedom in path planning is not optimal in terms of safety for higher densities [14]. In that study, several unmanaged en route airspace concepts, which varied in terms of the number of constrained degrees of motion, were compared qualitatively using simulation experiments. The results clearly showed that a layered airspace concept, which used a vertical segmentation of airspace to separate traffic with different travel directions at different flight levels, led to the highest safety. The increased safety for 'layers' was found to be a result of the reduction of relative velocities between cruising aircraft at the same altitude, which in turn reduced the number of conflicts when compared to a completely unstructured airspace design.

Using the qualitative understanding gained from [14] as a starting point, the current paper aims to develop quantitative models that describe the intrinsic safety provided by unstructured and layered en route airspace designs. Here the notion of intrinsic safety refers to the ability of an airspace design to reduce the occurrence of conflicts due to the constraints that it imposes on traffic motion. As such, the intrinsic safety provided by an airspace design is irrespective of whether or not conflicts are actually detected by aircraft; instead this aspect of safety considers the effect of the route structure imposed by a particular design on the number of 'truly occurring' conflicts. Consequently, intrinsic safety is directly proportional to the workload experienced by pilots and/or air traffic controllers in resolving any remaining conflicts that could not be prevented by a particular airspace design.

The modeling approach used in this work treats aircraft conflicts similar to the collisions that occur between ideal gas particles to determine instantaneous system-wide conflict counts as a measure of intrinsic safety. In comparison to previous studies, the models considered here take into account the effect of the horizontal *and* the vertical motion of aircraft on conflict counts. This is done by grouping the considered aircraft according to flight phase, while also considering the proportion of aircraft in different flight phases. This approach allows conflicts involving climbing and descending traffic, as well as those between aircraft, to be taken into account. Because the resulting three-dimensional analytical models use measurable airspace characteristics, such as traffic demand and separation requirements, as inputs, they lend themselves well for airspace design applications as the interactions between the factors affecting safety can be directly understood from the structure of the models. Moreover, their analytical nature makes it possible to easily compare different airspace concepts, and to also fine-tune the parameters of the selected airspace design.

To assess the accuracy of the derived models, three separate fast-time simulation experiments have been performed, encompassing almost three million flights. The first experiment measures the accuracy of the models under ideal conditions, and analyzes the effect of the allowed heading range per flight level on the intrinsic safety of layered airspace concepts. The second experiment studies the effect of the proportion of aircraft in different flight phases on safety and on model accuracy. The final experiment focuses on the sensitivity of the models to a simplification made during the derivation process regarding the speed distributions of aircraft.

This paper begins with an outline of the relevant background material and an overview of previous research in section 2. Next, in sections 3 and 4, the derivation of the models is presented. This is followed by the design of the simulation experiments used to assess model accuracy in section 5. Simulation results are presented in section 6, and discussed in section 7. Finally, a summary of the main conclusions is given in section 8.

2. Background

This section summarizes the background material needed to follow the conflict count model derivations developed in this paper. The sections begins by discussing the relationship between conflicts and intrinsic airspace safety. Additionally, descriptions of the conceptual design of unstructured and layered airspace concepts, as well as a review of previous studies that have used analytical models to measure intrinsic airspace safety, are provided.

2.1. Conflicts, Intrusions and Intrinsic Airspace Safety

Safety in ATM is often measured in terms of the number of intrusions and conflicts. Here, intrusions, also known as losses of separation, occur when minimum separation requirements are violated. Conflicts, on the other hand, are

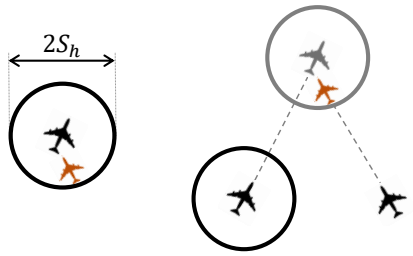

(a) Intrusion **(b) Conflict**

Figure 1: The difference between intrusions and conflicts, displayed here for the horizontal plane. Intrusions are violations of separation requirements, whereas conflicts are predicted intrusions. Here, S_h is the horizontal separation requirement.

defined as *predicted* intrusions; they occur when the horizontal and vertical distances between aircraft are expected to be less than the prescribed separation standards within a predetermined 'look-ahead' time. Therefore, when a conflict occurs, some action needs to be taken by pilots and/or air traffic controllers to prevent that conflict from turning into an intrusion in the future. The distinction between intrusions and conflicts is illustrated in Figure 1.

Although a conflict is strictly speaking only defined between two aircraft, they can also occur between with more aircraft at the same time. Such 'multi-aircraft' conflicts can still be treated as several two-aircraft conflicts and are included in the number of combinations based only on pairs of aircraft. For example, a multi-aircraft conflict involving four aircraft can result in *up to* six unique two-aircraft conflicts; see Figure 2. This combinatorial property is used by the modeling approach described in this work, see section 2.4.

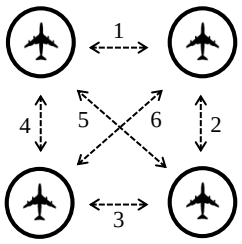

Figure 2: A multi-aircraft conflict can be decomposed into several two-aircraft conflicts. For example, a multi-aircraft conflict between four aircraft can result in up to six unique two-aircraft conflicts.

As mentioned earlier, this work focuses on modeling the *intrinsic safety* of unstructured and layered airspaces. The notion of intrinsic safety focuses exclusively on the safety that is provided by the constraints imposed on aircraft motion by an airspace design. Since the type and number of constraints imposed directly affects the probability of intersecting trajectories, the intrinsic safety of an airspace design can be measured in terms of the number of conflicts that occur at any given moment in time, i.e., by the number of instantaneous conflicts. Although measurement and communication uncertainties can affect the number of observed, or perceived, conflicts for particular a aircraft, such uncertainties are unrelated to the design of an airspace. As such, the intrinsic safety provided by an airspace design is only concerned with the 'truly occurring' conflicts in an airspace.

Because intrinsic safety considers the situation *without* tactical conflict resolution, it can be used as an indication of the workload that is experienced by pilots and/or air traffic controllers in solving conflicts under the considered airspace concept. It can also be used to analyze the frequency of conflicts that any future automated conflict resolution system should be able to handle. This flexibility allows the methods discussed in this paper to be applied to current commercial air traffic operations, as well as for future operations integrating unmanned aircraft with automated detect-and-avoid systems.

2.2. Unstructured Airspace

As the name suggests, no constraints are imposed on aircraft motion in Unstructured Airspace (UA). Instead, this simplest form of airspace design focuses on maximizing overall system efficiency. Therefore, aircraft are free to use direct horizontal routes, as long as such routing is not obstructed by weather or static obstacles. Similarly, aircraft can also fly with preferred speeds and at optimum altitudes, based on their performance capabilities and trip distances. By offering greater freedom to aircraft operators, UA has been found to result in a more uniform distribution of traffic, both horizontally and vertically, reducing traffic concentrations and ensuing delays [8, 15].

2.3. Layered Airspace

Several different layered airspace concepts have been discussed in literature [16, 17, 18]. The specific variation under consideration in this work was developed in our prior work [14], and is known as the 'Layers' concept.

The Layers concept can be seen as an extension to the hemispheric/semicircular rule [19]. In this concept, the airspace is segmented into vertically stacked bands, and heading-altitude rules are used to limit the range of travel directions allowed in each altitude layer. Although the Layers concept dictates the vertical profile of a flight, operators are free to select direct horizontal routes when possible. Moreover, climbing and descending aircraft are exempted from the heading-altitude rules, and can violate them to reach their cruising altitude or destination. This exception avoids inefficient 'spirals' when climbing/descending.

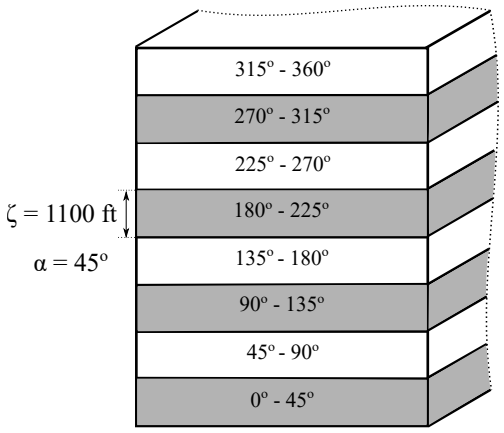

Figure 3: Isometric view of an example Layers concept, with an allowed heading range of $\alpha = 45^o$ per flight level, and a vertical spacing of $\zeta = 1100$ ft between flight levels

An example Layers concept is shown in Figure 3. Two parameters define the topology of the Layers concept. The first parameter is the spacing between altitude bands, ζ. An important design requirement is that ζ is *at least* equal to the vertical separation requirement to prevent conflicts between aircraft cruising in adjacent flight levels. In this work, a vertical separation requirement of 1000 ft is used. Therefore, the altitude bands of the Layers concepts considered here are separated by $\zeta = 1100$ ft; the extra 100 ft is used to prevent so called 'false' conflicts that can sometimes occur due to any slight overshooting of altitude when aircraft level-off at their desired flight level. Such an offset is also necessary to account for any height-keeping errors, and because of turbulence.

The second design parameter of the Layers concept is the heading range allowed per altitude band, α. For the layered airspace shown in Figure 3, $\alpha = 45^o$, and thus eight flight levels are needed to define one complete 'set' of layers. Correspondingly, for a layered design with $\alpha = 90^o$, only four flight levels would be needed to specify all possible travel directions. Therefore, for $\alpha = 90^o$, two complete 'sets' of layers would fit within the volume of airspace needed for $\alpha = 45^o$. When multiple sets of layers are available, the total trip distance of an aircraft is used in addition to its heading to determine its cruising altitude. In this way, short flights can use lower layer sets, and longer flights can use higher layer sets, to reduce the negative effect of predetermined altitudes on flight efficiencies.

2.4. Previous Research on Conflict Count Modeling

To model the total number of instantaneous conflicts in a given volume of airspace, it is necessary to take into account the total number of possible interactions between aircraft in that airspace, i.e., the maximum number of unique, two-aircraft combinations. Since any conflict can be decomposed into a series of one or more two-aircraft conflicts, see section 2.1, the maximum number of instantaneous conflicts possible is equal to the total number of unique two-aircraft combinations. However, in practice, not all aircraft are likely to be in conflict at the same time because the distance between corresponding aircrafts may be too large, or because the constraints imposed by a particular airspace design may prevent the trajectories of two specific aircraft from ever intersecting. Consequently, the total number of instantaneous conflicts can be estimated by scaling the *number of combinations of two aircraft* with the *average probability of conflict between any two aircraft*. This can be expressed in words as:

$$\begin{aligned} \text{No. Instantaneous Conflicts} = {} & \text{No. of Combinations of Two Aircraft} \\ & \times \\ & \text{Average Conflict Probability Between Any Two Aircraft} \end{aligned} \tag{1}$$

Here, different airspace designs can influence both the number of possible combinations of aircraft and the average conflict probability between any two aircraft.

In previous literature, this combinatorial characteristic, which is inherent to any system where all moving particles are equally likely to meet each other, has often been referred to as the 'gas model' since collisions between molecules in an ideal gas adhere to the same principle [20]. In the field of ATM, such models were first used to analyze the collision risk between adjacent routes of the North Atlantic track system [21, 22, 23]. Subsequently, they have also been used to investigate the safety of a wide variety of airspace types, including high altitude en route airways [24, 25, 26], low altitude terminal airspaces [27, 28, 29, 30], and for concepts that closely resemble unstructured and layered airspace concepts [31, 32, 33].

An important step in the derivation of a conflict model for a specific airspace design is the modeling of the *expected relative velocity* between aircraft, as this is needed to compute the average conflict probability between aircraft. Since aircraft move relative to each other in three-dimensional space, it is necessary to consider both the horizontal *and* vertical components of the relative velocity between aircraft. However, as most previous studies have only considered interactions between cruising aircraft, they have only presented models for the horizontal component of the expected relative velocity. Although a few studies have included climbing/descending traffic, they have done so by assuming a uniform distribution of flight-path angles, without adequate explanations for the distribution shape or the range of values selected [31, 27]. Moreover, a uniform distribution of flight-path angles is not a reasonable assumption for en route airspace design, the focus of the current paper. This is particularly the case for layered airspace designs which require aircraft to maintain fixed altitudes while cruising, see section 2.3. Consequently, the distribution of flight-path angles can be skewed, and depends on the proportion of aircraft in different flight phases.

Building on our earlier work [33], this paper extends previous research on conflict count modeling, by developing analytical models for both the horizontal *and* vertical components of the expected relative velocity. While the derivation of the former is comparable to that in previous literature, a grouping of aircraft flight segments into climbing, cruising and descending phases is used in this paper for the vertical direction. Consequently, the models derived here compute the total three-dimensional conflict probability as a function of the proportion of aircraft in different flight phases. This makes it possible to study how the proportion of cruising aircraft affects safety, or equally how the proportion of climbing/descending traffic affects safety. Conflicts involving climbing/descending aircraft are of particular interest to layered airspace designs, where constraints are imposed to only reduce conflicts between cruising aircraft.

In addition to extending the models to three dimensions, this paper also presents extensive fast-time simulation experiments to test model accuracy for a wide variety of conditions. This includes an investigation of an assumption made during the derivation process regarding the speed distribution of aircraft. Additionally, it is also shown how a numerical method can be used to augment the analytical models to further improve accuracy for cases where the speed distribution of aircraft violates modeling simplifications.

3. Modeling Conflict Probability

The goal of this section is to derive conflict probability expressions for direct-routing airspace concepts, such as unstructured and layered airspace designs, as a function of conflict detection parameters. Here, the conflict probability of an airspace design is defined as the likelihood that two randomly selected aircraft are in conflict, i.e., the likelihood that the trajectories of two arbitrary aircraft are predicted to be closer than the prescribed separation requirements within the conflict detection look-ahead time. Although the main contribution of this study is on the development of 3D conflict probability models, this section begins by considering the 2D case. This is because the 2D model is directly required to estimate conflict counts between cruising aircraft in layered airspaces. The 3D model is subsequently derived as an extension of the 2D case.

3.1. Conflict Probability for 2D Airspace

In 2D airspace, aircraft motion is restricted to the horizontal plane. Thus, aircraft velocities are purely horizontal, and all conflicts are between cruising aircraft.

Previous studies have proposed that the conflict probability between any two aircraft in 2D airspace, p_{2d}, can be computed by comparing the instantaneous *area searched* for conflicts by an aircraft, A_c, to the *total airspace area* under consideration, A_{total}; see Figure 4. Here it can be seen that A_c is approximated as a rectangular 'conflict search area', and its size is defined by the conflict detection look-ahead time, t_l, the horizontal separation requirement, S_h, and the expected horizontal relative velocity between aircraft, $\mathbf{E}\left(V_{r,h}\right)$. Since a conflict is detected if the trajectory of another aircraft is predicted to pass through A_c, p_{2d} can be expressed as [27, 28, 30]:

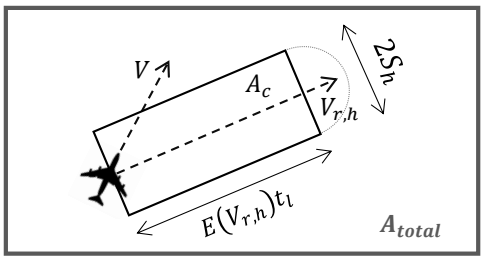

Figure 4: Area searched for conflicts, A_c, in 2D airspace. Here, A_{total} is the total airspace area under consideration.

$$p_{2d} = \frac{A_c}{A_{total}} = \frac{2\ S_h\ \mathbf{E}\left(V_{r,h}\right)\ t_l}{A_{total}} \tag{2}$$

To arrive at a fully analytical expression for p_{2d}, it is necessary to quantify $\mathbf{E}\left(V_{r,h}\right)$. Because the goal of the derivation process is to determine the average conflict probability between a population of aircraft for a given airspace design, and not just between two specific flights, the *expected* horizontal relative velocity is used. More specifically, $\mathbf{E}\left(V_{r,h}\right)$ can be thought of as the weighted average of the horizontal relative velocities between *all* aircraft pairs (not just the conflicting pairs), given the aircraft speed and heading difference distributions in the airspace area of interest.

Nonetheless, to compute $\mathbf{E}\left(V_{r,h}\right)$, it is still useful to first consider the magnitude of the horizontal relative velocity between an arbitrary pair of aircraft, $V_{r,h}$; see Figure 5. Using the cosine rule, $V_{r,h}$ can be computed as:

$$V_{r,h} = \left(V_1^2 + V_2^2 - 2V_1V_2\cos\left(\Delta\psi\right)\right)^{1/2} \tag{3}$$

Here, V_1 and V_2 are the velocity magnitudes of the two aircraft pictured in Figure 5, and $\Delta\psi$ is the heading difference between these two arbitrary aircraft. Because the values of these variables can be different for every aircraft pair in the airspace, it is necessary to integrate equation 3 over all possible values of velocity and heading difference to compute $\mathbf{E}\left(V_{r,h}\right)$, while taking into account the probability density functions of velocity magnitudes and heading differences, $P\left(V_1\right)$, $P\left(V_2\right)$ and $P\left(\Delta\psi\right)$:

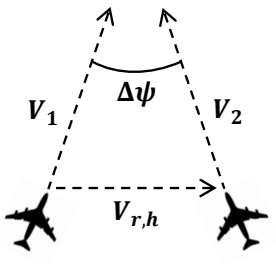

Figure 5: The geometric relationships between velocity, V, relative velocity, V_r, and heading difference $\Delta\psi$ for two arbitrary aircraft

$$\mathbf{E}\left(V_{r,h}\right) = \int_{V_1}\int_{V_2}\int_{0}^{\alpha} \left(V_1^2 + V_2^2 - 2V_1V_2\cos\left(\Delta\psi\right)\right)^{1/2} \; P\left(\Delta\psi\right)P\left(V_1\right)P\left(V_2\right) \; d\Delta\psi \, dV_1 \, dV_2 \tag{4}$$

In the above equation, α represents the maximum possible heading difference between any two cruising aircraft. Due to the complexity of equation 4, it can only be solved numerically [27]. However, an analytical solution is possible if all aircraft are assumed to have equal velocity magnitudes, i.e., if $V_1 = V_2 = V_o$. Under this assumption, the geometry between V_1, V_2 and $V_{r,h}$ in Figure 5 becomes an isosceles triangle. Thus, it is possible to rewrite equation 3 as:

$$V_{r,h} = 2\,V_o\,\sin\left(\frac{|\Delta\psi|}{2}\right) \tag{5}$$

Since V_o is assumed to be a constant, the above simplified equation shows that $V_{r,h}$ is only dependent on the absolute heading difference between two aircraft, $|\Delta\psi|$. Therefore a simplified analytical expression for $\mathbf{E}\left(V_{r,h}\right)$ can be derived by integrating equation 5 for all possible $|\Delta\psi|$, while taking into account its probability density. In order to highlight the safety differences between unstructured and layered airspaces, traffic scenarios with a uniform distribution of aircraft headings between 0 and α are used in this work, since such scenarios have been shown in literature to maximize conflict counts [27]. For this type of scenario, the probability density function of the absolute heading difference, $P\left(|\Delta\psi|\right)$, takes on a triangular shape between 0 and α [34]:

$$P\left(|\Delta\psi|\right) = \frac{2}{\alpha}\left(1 - \frac{|\Delta\psi|}{\alpha}\right) \tag{6}$$

Using equations 5 and 6, a simplified expression for $\mathbf{E}\left(V_{r,h}\right)$ can be determined as [33]:

$$\begin{aligned}\mathbf{E}\left(V_{r,h}\right) &= \int_0^{\alpha} 2V_o \sin\left(\frac{|\Delta\psi|}{2}\right)\cdot\frac{2}{\alpha}\left(1-\frac{|\Delta\psi|}{\alpha}\right)\; d\,|\Delta\psi| \\ &= \frac{8V_o}{\alpha}\left(1 - \frac{2}{\alpha}\sin\frac{\alpha}{2}\right)\end{aligned} \tag{7}$$

It should be noted that the above expression is only valid if all aircraft are assumed to have equal velocities. This assumption is used for all the analytical models derived in this paper, and by all previous studies that have developed *analytical* conflict count models to analyze the safety of a particular airspace design, see section 2.4. Nevertheless, the sensitivity of this assumption on model accuracy is specifically analyzed by one of the fast-time simulation experiments performed in this work, see section 6.3.

3.2. Conflict Probability for 3D Airspace

In 3D en route airspace, cruising aircraft share the airspace with climbing and descending aircraft. Therefore in 3D, conflicts can occur between aircraft in different flight phases. Moreover, aircraft can have horizontal, as well as vertical velocity components.

Analogous to the two-dimensional case, for 3D airspace, conflict probability can be defined as the ratio between the instantaneous *volume* of airspace searched for conflicts, B_c, and the total airspace volume under consideration B_{total}; see Figure 6(a). Furthermore, a conflict is defined to occur when the trajectory of another aircraft is predicted to pass through B_c, and its size is dependent on the conflict detection look-ahead time, t_l, the horizontal and vertical separation requirements, S_h and S_v, and the expected relative velocity, $\mathbf{E}\left(V_r\right)$.

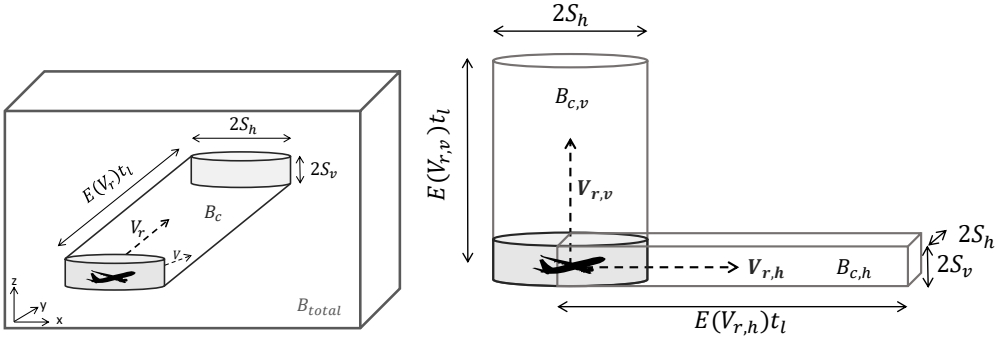

(a) Volume searched for conflicts, B_c

(b) Horizontal and vertical components of volume searched for conflicts, $B_{c,h}$ and $B_{c,v}$

Figure 6: Volume searched for conflicts by an aircraft, B_c, in 3D airspace. Here, B_{total} is the total volume of the airspace consideration. Note that $B_c = B_{c,h} + B_{c,v}$

It can be shown that volume B_c can be decomposed into two orthogonal components:

1. A horizontal cuboid, $B_{c,h}$, generated by the horizontal component of the expected relative velocity, $\mathbf{E}\left(V_{r,h}\right)$
2. A vertical cylinder, $B_{c,v}$, generated by the vertical component of the expected relative velocity, $\mathbf{E}\left(V_{r,v}\right)$

The horizontal and vertical components of B_c can be visualized in Figure 6(b). Because $B_c = B_{c,h} + B_{c,v}$, the total 3D conflict probability, p_{3d}, can be modeled as a summation of the horizontal and vertical 'volume searched' ratios:

$$p_{3d} = \frac{B_c}{B_{total}} = \frac{B_{c,h} + B_{c,v}}{B_{total}} = \frac{4\, S_h S_v\, \mathbf{E}\left(V_{r,h}\right) t_l + \pi S_h^2\, \mathbf{E}\left(V_{r,v}\right) t_l}{B_{total}} \tag{8}$$

To fully quantify p_{3d}, it is necessary to develop analytical formulations for the expected horizontal and vertical relative velocities. This is done in the following paragraphs.

3.2.1. Expected Horizontal Relative Velocity

To model the expected horizontal relative velocity in an airspace, $\mathbf{E}\left(V_{r,h}\right)$, it is first necessary to properly define what is meant as the 'horizontal velocity' of an aircraft, V_h; see Figure 7. This figure shows that V_h is a function of the of the total velocity of an aircraft, V, and its flight-path angle, γ :

$$V_h = V \cos\left(\gamma\right) \tag{9}$$

As indicated previously, this paper is concerned with modeling conflict counts for *en route* airspace. In en route airspace, aircraft generally climb/descend with flight-path angles less than six degrees. Based on the above equation, for such small angles, $V_h \approx V$. Therefore γ does *not* significantly affect V_h in en route airspace. For this reason, $V_{r,h}$

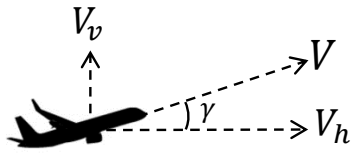

Figure 7: The flight path angle of an aircraft, γ, is defined in terms of its horizontal velocity, V_h, and its vertical velocity, V_v.

and $\mathbf{E}(V_{r,h})$ can also be considered to be independent of γ in en route airspace. Thus, the expression for $\mathbf{E}(V_{r,h})$ developed earlier for 2D en route airspace, given by equation 7, can also be used for 3D en route airspace.

It is important to note that the approach presented here to model $\mathbf{E}(V_{r,h})$ is only applicable for small flight-path angles, as is the case in en route airspaces. For the rare cases where $\gamma >> 10^o$, it would be necessary to take γ into account when computing $\mathbf{E}(V_{r,h})$. This would require a rewriting of equations 4 and 7 to include an additional integral that considers the probability density of γ when modeling $\mathbf{E}(V_{r,h})$. However, as shown by the high model accuracy results in section 6, this added complexity is generally not required.

3.2.2. Expected Vertical Relative Velocity

Following a similar procedure to the horizontal direction, it is useful to first define the vertical velocity of an individual aircraft, V_v. Using Figure 7, V_v can be computed as:

$$V_v = V \sin(\gamma) \tag{10}$$

For small values of γ, as for en route airspace, the above equation can be simplified as $V_v \approx V\gamma$. Therefore, unlike the horizontal case, V_v is dependent on γ. If all aircraft are assumed to have equal total velocities, i.e., if $V = V_o$, then the magnitude of the vertical relative velocity between two arbitrary aircraft, $V_{r,v}$, is dependent on the flight path angles of each aircraft, γ_1 and γ_2:

$$V_{r,v} = |V_o \sin(\gamma_2) - V_o \sin(\gamma_1)| \tag{11}$$

Because the values of γ_1 and γ_2 can be different for every aircraft pair, to compute the expected vertical relative velocity, $\mathbf{E}(V_{r,v})$, it is necessary to integrate equation 11 for all possible values of γ_1 and γ_2, while taking into account the probability density function of the flight path angles of each aircraft, $P(\gamma_1)$ and $P(\gamma_2)$:

$$\mathbf{E}(V_{r,v}) = \int_{\gamma_1}\int_{\gamma_2} |V_o \sin(\gamma_2) - V_o \sin(\gamma_1)| \; P(\gamma_1) P(\gamma_2) \; d\gamma_1 \, d\gamma_2 \tag{12}$$

To develop an analytical model for $\mathbf{E}(V_{r,v})$, the following simplification is made in this paper. In en route airspace, an aircraft can be considered to be either cruising or climbing or descending. Cruising aircraft generally fly with $\gamma_{cruise} \approx 0^o$. Furthermore, it is reasonable to assume a constant and equal $|\gamma|$ for all climbing and descending aircraft. Therefore, it is assumed that γ takes one of the following three values in en route airspace:

$$\gamma = \begin{cases} 0 & \text{for cruising aircraft} \\ +\gamma_{cd} & \text{for climbing aircraft} \\ -\gamma_{cd} & \text{for descending aircraft} \end{cases} \tag{13}$$

Using the above simplification, it is possible to rewrite equation 12 into its discretized form:

$$\mathbf{E}(V_{r,v}) = \sum_{\gamma_1}\sum_{\gamma_2} |V_o \sin(\gamma_2) - V_o \sin(\gamma_1)| \; P(\gamma_1) P(\gamma_2) \tag{14}$$

To utilize equation 14, it is necessary to determine discretized values for $V_{r,v}$ and $P(\gamma_1) \cdot P(\gamma_2)$. Discretized values of $V_{r,v}$ can be computed by evaluating equation 11 for all flight phase combinations of two arbitrary aircraft, see Table 1. This table shows that $V_{r,v}$ is zero when both aircraft have the same flight path angle, and that $V_{r,v}$ is highest when the two aircraft are flying with opposite flight path angles, as expected.

Table 1: Discretized vertical relative velocity, $\mathbf{V_{r,v}}$

AC 1 \ AC 2	Cruising	Climbing	Descending
Cruising	0	$V_o \sin(\gamma_{cd})$	$V_o \sin(\gamma_{cd})$
Climbing	$V_o \sin(\gamma_{cd})$	0	$2V_o \sin(\gamma_{cd})$
Descending	$V_o \sin(\gamma_{cd})$	$2V_o \sin(\gamma_{cd})$	0

Discretized values for $P(\gamma_1) \cdot P(\gamma_2)$ can be computed by noting that the discretized probability distribution of γ is equivalent to the proportion of aircraft in cursing, climbing and descending flight phases. To this end, let ε be the proportion of cruising aircraft:

$$\varepsilon = \frac{N_{cruise}}{N_{total}} \tag{15}$$

Here, N_{cruise} is the number of instantaneous cruising aircraft, and N_{total} is the total number of instantaneous aircraft. Using ε, the proportion of climbing or descending aircraft can calculated be as $1 - \varepsilon$, and the probability of selecting two cruising aircraft at random is ε^2. Using this approach, the discretized values for $P(\gamma_1) \cdot P(\gamma_2)$ can be computed for all flight phase combinations of two arbitrary aircraft, see Table 2. Because this table represents a discrete probability density function, summation of the cells lead to a value of 1. Moreover, the table is symmetric along the leading diagonal as it assumes equal numbers of climbing and descending aircraft, which was in turn used to simplify the design of the simulation experiments, see section 5. However, the method described here can also be applied when this assumption is not true, as long as the proportion of aircraft in different flight phases are known.

Table 2: Discretized flight-path angle probability density distribution, $\mathbf{P}(\gamma_1) \cdot \mathbf{P}(\gamma_2)$

AC 1 \ AC 2	Cruising	Climbing	Descending
Cruising	ε^2	$\frac{\varepsilon - \varepsilon^2}{2}$	$\frac{\varepsilon - \varepsilon^2}{2}$
Climbing	$\frac{\varepsilon - \varepsilon^2}{2}$	$\frac{(1-\varepsilon)^2}{4}$	$\frac{(1-\varepsilon)^2}{4}$
Descending	$\frac{\varepsilon - \varepsilon^2}{2}$	$\frac{(1-\varepsilon)^2}{4}$	$\frac{(1-\varepsilon)^2}{4}$

Using equation 14 and the discretized values for $V_{r,v}$ and $P(\gamma_1) \cdot P(\gamma_2)$ in Tables 1 and 2, respectively, $\mathbf{E}(V_{r,v})$ can be computed. In essence, this involves an element-wise multiplication of the appropriate cells of Tables 1 and 2, followed by a summation of the resulting expressions. Since this process has to take into account the allowed flight phase combinations of interacting aircraft, the resulting $\mathbf{E}(V_{r,v})$ expressions are different for unstructured and layered airspace designs; the corresponding equations are derived in sections 4.1 and 4.2, respectively.

4. Modeling Conflict Counts

This section presents the derivation of conflict count models for unstructured and layered airspace concepts. These derivations make use of the 2D and 3D conflict probability models developed in the previous section, and are adaptations of the generic conflict count model given by equation 1.

4.1. Unstructured Airspace

As indicated by equation 1, the number of instantaneous conflicts for Unstructured Airspace (UA), C_{ua}, can be modeled as the product of two factors, namely the *number of combinations of two aircraft*, and the *conflict probability between any two aircraft*. Because UA imposes no constraints on aircraft motion, an aircraft can conflict with any other aircraft in the airspace, regardless of the flight phase of either aircraft. Therefore, the total number of combinations of two aircraft can be expressed using the binomial coefficient, $\binom{N_{total}}{2}$, leading to the following model structure for C_{ua}:

$$C_{ua} = \binom{N_{total}}{2} p_{ua} = \frac{N_{total}\left(N_{total}-1\right)}{2} p_{ua} \tag{16}$$

Here, N_{total} is the total number of instantaneous aircraft present in the volume of airspace under consideration. The conflict probability between any two aircraft, p_{ua}, scales the number of combinations of two aircraft such that only aircraft pairs that have intersecting trajectories within detection range are counted as conflicts. A model for conflict probability in 3D airspaces has been derived in section 3.2. It is repeated below for convenience, and uses the geometrical parameters defined in Figure 6:

$$p_{ua} = \frac{4\, S_h S_v\, \mathbf{E}\left(V_{r,h}\right) t_l + \pi S_h^2\, \mathbf{E}\left(V_{r,v}\right) t_l}{B_{total}} \tag{8}$$

To evaluate the above equation, expressions for the expected horizontal and vertical relative velocities between aircraft in UA, $\mathbf{E}\left(V_{r,h}\right)_{ua}$ and $\mathbf{E}\left(V_{r,v}\right)_{ua}$, are needed. Equation 7 shows that $\mathbf{E}\left(V_{r,h}\right)_{ua}$ is dependent on α, the maximum possible heading difference between two arbitrary aircraft. Since aircraft have complete route selection freedom in UA, conflicts can occur between aircraft flying in any direction. Thus for UA, $\alpha = 360^o = 2\pi$. Substitution of this value into equation 7 yields the following expression for $\mathbf{E}\left(V_{r,h}\right)_{ua}$:

$$\mathbf{E}\left(V_{r,h}\right)_{ua} = \frac{4V_o}{\pi} \tag{17}$$

Here, V_o is the assumed equal velocity of all aircraft in the airspace. As mentioned before, the effect of this assumption on model accuracy is analyzed using fast-time simulations, see section 6.3.

In the vertical direction, equation 14 can be used to compute $\mathbf{E}\left(V_{r,v}\right)_{ua}$. To use equation 14, expressions for the discretized vertical relative velocity, and the discretized flight-path angle probability density distribution, listed in Tables 1 and 2, respectively, are needed. Since the probability of conflict is independent of flight phase in UA, the expressions for all flight phases in Tables 1 and 2 should be used when evaluating equation 14. This results in the following for UA:

$$\begin{aligned}\mathbf{E}\left(V_{r,v}\right)_{ua} &= 4\left(V_o \sin\left(\gamma_{cd}\right) \frac{\varepsilon-\varepsilon^2}{2}\right) + 2\left(2V_o \sin\left(\gamma_{cd}\right) \frac{\left(1-\varepsilon\right)^2}{4}\right) \\ &= V_o \sin\left(\gamma_{cd}\right)\left(1-\varepsilon^2\right)\end{aligned} \tag{18}$$

Here, γ_{cd} is the flight-path angle of climbing/descending traffic, and ε is the proportion of cruising aircraft in the airspace. Finally, the number of instantaneous conflicts for UA can be obtained by substituting equations 17 and 18 into equation 8, and then substituting the result into equation 16:

$$C_{ua,3d} = \frac{N_{total}\left(N_{total}-1\right)}{2}\left(\frac{16\ S_h S_v V_o t_l + \pi^2 S_h^2 V_o t_l \sin\left(\gamma_{cd}\right)\left(1-\varepsilon^2\right)}{\pi\ B_{total}}\right) \tag{19}$$

4.2. Layered Airspace

The structure of the Layers concept reduces the number of conflicts between cruising aircraft. However, there are no procedural mechanisms to separate cruising aircraft from climbing and descending traffic. Therefore, the conflict count model for layered airspaces needs to be split into three distinct parts based on the flight phase combinations of interacting aircraft:

$$C_{lay} = C_{cruise} + C_{cruise-cd} + C_{cd} \tag{20}$$

Here, C_{cruise} is the number of conflicts between cruising aircraft, $C_{cruise-cd}$ is the number of conflicts between cruising and climbing/descending aircraft, and C_{cd} is the number of conflicts between climbing/descending traffic. Each of these three conflict types are discussed in the paragraphs that follow.

4.2.1. Conflicts Between Cruising Aircraft

The number of instantaneous conflicts between cruising aircraft in the Layers concept can be modeled by taking into account the two aspects that differentiate layered airspaces from UA; the reduction of the number of possible conflict pairs, and the reduction of the relative velocity between cruising aircraft.

Conflict Pair Reduction

Since the vertical spacing between the predefined flight levels of the Layers concept is by definition at least equal to the vertical separation requirement, cruising aircraft at different altitude bands can not conflict with each other. This in turn reduces the number of possible conflict pairs for cruising aircraft. It also means that the conflict probability between cruising aircraft, p_{cruise}, is equal for all cruising flight levels. Thus, in a single flight level j, the number of conflicts between cruising aircraft, $C_{cruise,j}$, can be expressed as:

$$C_{cruise,j} = \frac{N_{cruise,j}\left(N_{cruise,j}-1\right)}{2}\ p_{cruise} \tag{21}$$

Here, $N_{cruise,j}$ is the number of cruising aircraft in flight level j. By summing equation 21 over all available flight levels, L, the total number of instantaneous cruising conflicts can be computed as:

$$C_{cruise} = \sum_{j}^{L} \frac{N_{cruise,j}\left(N_{cruise,j}-1\right)}{2}\ p_{cruise} \tag{22}$$

If cruising aircraft are uniformly distributed over all altitude bands, then $N_{cruise,j} = N_{cruise}/L$. This would be the case for layered airspaces if aircraft headings are also uniformly distributed, as for the traffic patterns considered in this work. In case of an uneven distribution of aircraft headings, a uniform vertical distribution of traffic can still be achieved by assigning multiple flight levels for the heading ranges with high demand. Using this assumption, equation 22 can be simplified to:

$$C_{cruise} = \frac{N_{cruise}\left(\frac{N_{cruise}}{L}-1\right)}{2}\ p_{cruise} \tag{23}$$

From the above equation, it can be concluded that increasing L increases the intrinsic safety offered by layered concepts to cruising aircraft. This is because higher values of L reduce the number of possible combinations of cruising aircraft pairs that can interact with each other.

Relative Velocity Reduction

As aircraft in the Layers concept are 'sorted' into different altitude bands based on their heading, the second beneficial effect of the Layers concept is the reduction of the expected horizontal relative velocities between cruising aircraft, $\mathbf{E}\left(V_{r,h}\right)_{cruise}$. A reduction of $\mathbf{E}\left(V_{r,h}\right)_{cruise}$ leads to a reduction of p_{cruise}, which in turn increases safety. Since cruising aircraft are constrained to the horizontal plane, the 2D conflict probability model derived in section 3.1 can be used for p_{cruise} and $\mathbf{E}\left(V_{r,h}\right)_{cruise}$. They are restated below for convenience, and use the geometrical parameters defined in Figure 4:

$$p_{cruise} = \frac{2\, S_h\, \mathbf{E}\left(V_{r,h}\right)_{cruise}\, t_l}{A_{total}} \tag{2}$$

$$\mathbf{E}\left(V_{r,h}\right)_{cruise} = \frac{8V_o}{\alpha}\left(1 - \frac{2}{\alpha}\sin\frac{\alpha}{2}\right) \tag{7}$$

Equation 7 shows that $\mathbf{E}\left(V_{r,h}\right)_{cruise}$ is a function of the heading range permitted per altitude band, α. As indicated in section 2.3, α is a design parameter for layered airspaces. To gain a sense of the effect of α on the safety of the Layers concept, equation 7 is plotted in Figure 8. Here it can be seen that the horizontal relative velocity varies non-linearly with α due to the $\sin\frac{\alpha}{2}$ term in equation 7. Furthermore, the figure shows that $\mathbf{E}\left(V_{r,h}\right)_{cruise}$ is lower for layered concepts with smaller values of α. Since reducing $\mathbf{E}\left(V_{r,h}\right)_{cruise}$ decreases p_{cruise}, reducing α is hypothesized to increase the intrinsic safety of layered concepts.

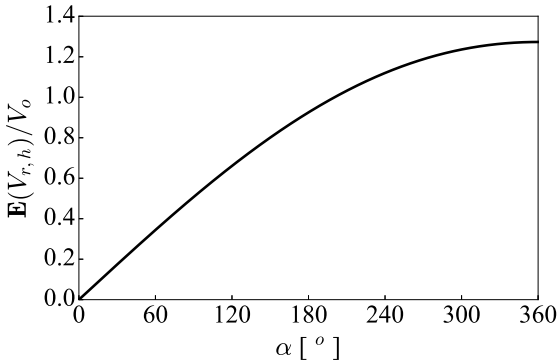

Figure 8: Hypothesized relationship between the expected horizontal relative velocity, $\mathbf{E}\left(V_{r,h}\right)$, and heading range per flight level, α

Substituting equations 2 and 7 into equation 23 leads to the following expression for the number of instantaneous conflicts between cruising aircraft in layered airspaces:

$$C_{cruise} = N_{cruise}\left(\frac{N_{cruise}}{L} - 1\right)\left(\frac{8\, S_h\, V_o\, t_l}{\alpha\, A_{total}}\right)\left(1 - \frac{2}{\alpha}\sin\frac{\alpha}{2}\right) \tag{24}$$

4.2.2. Conflicts Between Cruising and Climbing/Descending Aircraft

Because the Layers concept imposes no procedural constraints to prevent conflicts between cruising and climbing/descending traffic, the model for $C_{cruise-cd}$ is very similar to the model developed for UA, except for two minor differences:

1. The number of combinations of cruising and climbing/descending aircraft is $N_{cruise}\, N_{cd}$. This is because an aircraft can not be cruising and climbing/descending at the same time.
2. Since only cruising-climbing/descending conflicts are considered, the calculation of the expected vertical relative velocity, $\mathbf{E}\left(V_{r,v}\right)_{cruise-cd}$, should only consider cases where one aircraft is cruising, while the other is climbing/descending. This can be achieved by evaluating equation 14 for the four cases in Tables 1 and 2 where one aircraft is cruising, and the other is climbing/descending.

Application of these changes to the UA model leads to the following expressions for $C_{cruise-cd}$. These equations make use of the geometrical parameters displayed in Figure 6:

$$C_{cruise-cd} = N_{cruise}\, N_{cd}\, p_{cruise-cd} \tag{25a}$$

$$p_{cruise-cd} = \frac{4\, S_h S_v\, \mathbf{E}\left(V_{r,h}\right)_{cruise-cd} t_l + \pi S_h^2\, \mathbf{E}\left(V_{r,v}\right)_{cruise-cd} t_l}{B_{total}} \tag{25b}$$

$$\mathbf{E}\left(V_{r,h}\right)_{cruise-cd} = \frac{4V_o}{\pi} \tag{25c}$$

$$\mathbf{E}\left(V_{r,v}\right)_{cruise-cd} = 4\left(V_o \sin\left(\gamma_{cd}\right) \frac{\varepsilon - \varepsilon^2}{2}\right) = 2V_o \sin\left(\gamma_{cd}\right)\left(\varepsilon - \varepsilon^2\right) \tag{25d}$$

4.2.3. Conflicts Between Climbing/Descending Aircraft

The model describing the number of instantaneous conflicts between climbing/descending traffic, C_{cd}, is also remarkably similar to that derived earlier for UA. In this case, the only difference is in the computation of the expected vertical relative velocity between climbing/descending aircraft, $\mathbf{E}\left(V_{r,v}\right)_{cd}$. An expression for $\mathbf{E}\left(V_{r,v}\right)_{cd}$ can be obtained by applying equation 14 for the four cases in Tables 1 and 2 where both interacting aircraft are climbing/descending. This approach leads to the following for expressions for C_{cd}. These equations make use of the geometrical parameters displayed in Figure 6:

$$C_{cd} = \frac{N_{cd}\left(N_{cd} - 1\right)}{2} p_{cd} \tag{26a}$$

$$p_{cd} = \frac{4\, S_h S_v\, \mathbf{E}\left(V_{r,h}\right)_{cd} t_l + \pi S_h^2\, \mathbf{E}\left(V_{r,v}\right)_{cd} t_l}{B_{total}} \tag{26b}$$

$$\mathbf{E}\left(V_{r,h}\right)_{cd} = \frac{4V_o}{\pi} \tag{26c}$$

$$\mathbf{E}\left(V_{r,v}\right)_{cd} = 2\left(2V_o \sin\left(\gamma_{cd}\right) \frac{\left(1-\varepsilon\right)^2}{4}\right) = V_o \sin\left(\gamma_{cd}\right)\left(1-\varepsilon\right)^2 \tag{26d}$$

5. Fast-Time Simulation Design

To test the accuracy of the conflict count models developed in this work, three fast-time simulation experiments, named the 'primary experiment' the 'flight-path angle experiment' and the 'ground speed experiment', were performed. This section describes the design of these three experiments.

5.1. Simulation Development

5.1.1. Simulation Platform

The BlueSky open-source ATM simulator was used as the simulation platform in this research. It was developed at the Delft University of Technology (TU Delft) using the Python programming language[1]. BlueSky has numerous features including the ability to simulate more than 5000 aircraft simultaneously, a suite of conflict detection and resolution algorithms, and extensive data logging functions. A complete overview of BlueSky is provided in [35].

[1]BlueSky can be downloaded from `https://github.com/ProfHoekstra/blueksy`

In order to simulate aircraft performance dynamics, BlueSky uses point-mass Aircraft Performance Models (APMs) that are similar in structure to Eurocontrol's well known Base of Aircraft Data (BADA) models. The main difference between these two approaches is that BlueSky uses openly available data to quantify the APMS. To simplify the simulations, all traffic was simulated using a Boeing 744 model. A full description of the BlueSky APMs, including their validation, can be found in [36].

BlueSky uses a simulated Flight Management System (FMS) to provide horizontal and vertical navigation capabilities, as well as for aircraft speed control. Similar to real aircraft, the simulated FMS tries to fly an aircraft at the requested Calibrated Airspeed (CAS) or Mach number, if that is within the performance capabilities of the aircraft type, which is in turn specified in the APMs for different parts of the flight envelope. Additionally, speed/heading changes occur while respecting the acceleration capabilities of aircraft.

5.1.2. Conflict Detection

In this study, the so called 'state-based' conflict detection method was used. This method predicts separation violations by linearly extrapolating aircraft positions over a predefined look-ahead time. Here, a look-ahead time of 5 minutes, as well as separation requirements of 5 nautical miles horizontally and 1000 ft vertically, were used.

As mentioned in section 2.4, the models derived in this paper are concerned with the intrinsic safety provided by unstructured and layered airspace designs. Since the notion of intrinsic safety focuses on the number of *truly occurring* conflicts as a function of airspace design, conflict detection was performed assuming perfect knowledge of aircraft states. For the same reason, the simulations were performed without tactical conflict resolutions.

5.1.3. Airspace Concepts and Concept Implementation

Unstructured Airspace (UA) and four layered airspace concepts, each with a different allowed heading range per flight level, α, were used in the fast-time simulations. Table 3 displays the properties of the considered airspace concepts, and also indicates which concepts were used in each of the three experiments performed in this study.

Table 3: Properties of the airspace concepts used in the three simulation experiments

Symbol	Name	Heading Range Per Layer, α	Number of Layer Sets, κ	Primary Expt.	Flight-Path Angle Expt.	Ground Speed Expt.
UA	Unstructured Airspace	-	-	✓	✓	✓
L360	Layers 360	360^o	8	✓	-	-
L180	Layers 180	180^o	4	✓	-	-
L90	Layers 90	90^o	2	✓	-	-
L45	Layers 45	45^o	1	✓	✓	✓

The airspace concepts were implemented into BlueSky by modifying its trajectory planning functions. While direct horizontal routes were used in both unstructured and layered airspaces, the method used to determine the cruising altitude of an aircraft differed between the two airspace designs. For UA, the cruising altitude of an aircraft, $Z_{ua,i}$, was directly proportional to its trip distance, D_i:

$$Z_{ua,i} = Z_{min} + \frac{Z_{max} - Z_{min}}{D_{max} - D_{min}} \ (D_i - D_{min}) \tag{27}$$

Here, Z_{min} and Z_{max} are the minimum and maximum altitudes allowed for cruising aircraft in the simulation. Comparably, D_{min} and D_{max} are the minimum and maximum trip distances of aircraft in the simulation. Since traffic scenarios with a uniform distribution of trip distances were used, equation 27 resulted in a uniform vertical distribution of traffic.

On the other hand, for the Layers concept, the cruising altitude of an aircraft, $Z_{lay,i}$, depends on both its heading, ψ_i, and its trip distance, D_i, as indicated by the following heading-altitude rule:

$$Z_{lay,i} = Z_{min} + \zeta \left[\left\lfloor \frac{D_i - D_{min}}{D_{max} - D_{min}} \kappa \right\rfloor \beta + \left\lfloor \frac{\psi_i}{\alpha} \right\rfloor \right] \tag{28}$$

Here, β is the number of flight levels needed to define one complete set of layers, and κ is the number of complete layer sets. These two parameters are defined as $\beta = 360^o/\alpha$ and $\kappa = L/\beta$, where L is the total number of available flight levels. Note that the second term of equation 28 computes the cruising altitude of an aircraft as an *integer multiple* of the vertical spacing between flight levels, ζ, using the the floor operator ('$\lfloor\ \rfloor$'). For all layered concepts in this study, $\zeta = 1100$ ft and $L = 8$. Correspondingly, for most layered concepts, $\kappa > 1$; see Table 3. For layered concepts with $\kappa > 1$, equation 28 uses trip distances to determine cruising altitudes such that short flights remain at lower altitudes, while longer flights use higher layer sets. This property, combined with traffic scenarios with a uniform distribution of trip distances and travel directions, resulted in a uniform of distribution of cruising aircraft over the eight predefined flight levels used by all layered concepts.

It should be noted that the only difference between the UA and L360 concepts is the use of predefined flight levels for cruising aircraft in L360, while any altitude could be selected by aircraft in UA. In fact, the L360 concept was specifically included in the simulations to investigate the effect of using fixed cruising flight levels while simultaneously allowing all possible headings in each flight level on intrinsic airspace safety.

5.2. Traffic Scenarios

5.2.1. Testing Region and Flight Profiles

A large three-dimensional en route sector was used as the physical environment for traffic simulations; see Figure 9. In the vertical dimension, the sector is divided into two parts; a 'transition zone' with a height of 4000 ft for climbing and descending traffic, and a 'cruising zone' with a height of 7700 ft. The eight predefined cruising flight levels for layered airspace concepts were within the latter zone (not shown).

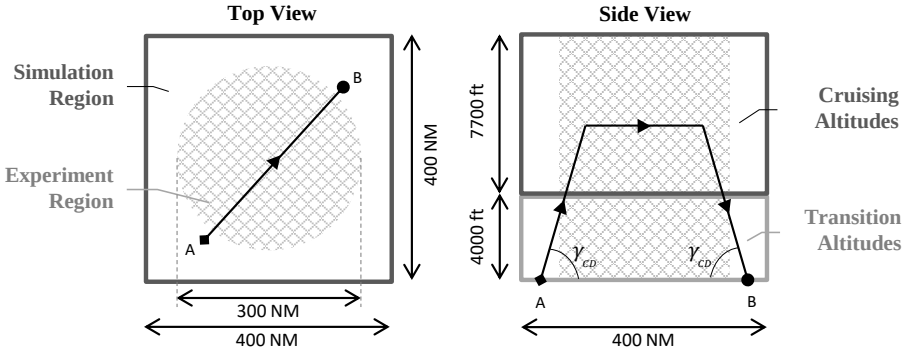

Figure 9: Top and side views of the simulation's physical environment. The trajectory of an example flight is shown.

In the horizontal plane, the sector had a square-shaped cross-section of 400 x 400 NM, and was divided into separate 'simulation' and 'experiment' regions; see Figure 9. As no traffic was simulated outside the square sector, aircraft near the edges of the 'simulation region' were unlikely to interact with other traffic compared to flights near the center of the sector. To solve this issue, following the simulation design in [11], a smaller cylindrical 'experiment region', with a diameter of 300 NM, was defined at the center of the simulation region. The resulting gap between the experiment and simulation regions, which was sized such that it closely matched the length of the *horizontal volume of airspace searched for conflicts* by aircraft, see Figure 6(b), ensures that aircraft in the experiment region are surrounded by traffic in all directions. Correspondingly, only aircraft within the experiment region, and only conflicts with closest points of approach with the experiment region, were used to assess the accuracy of the models. The parameters of the experiment region needed to evaluate the models, as well as other parameters common to all three experiments, are listed in Table 4.

Figure 9 also shows the horizontal and vertical profiles of an example flight. Because the focus of this study is on en-route airspace design, take-off and landing flight phases were not considered. Instead, aircraft entered the simulation

Table 4: Common simulation parameters for all three experiments

Parameter	Value	Description
A_{total}	7.0685·10^4 NM^2	Area of 'experiment region'
B_{total}	3.0533·10^{16} ft ^{3}	Volume of 'experiment region'
D_{min}	200 NM	Minimum trip distance
D_{max}	250 NM	Maximum trip distance
$\bar{D}$	225 NM	Average trip distance
t_l	5 mins	Conflict detection look-ahead time
S_h	5 NM	Horizontal separation requirement
S_v	1000 ft	Vertical separation requirement
L	8	Number of flight levels for layered airspaces
$\bar{V}$	400 kts	Average ground speed of aircraft

Table 5: Flight-path angle of climbing/descending aircraft (γ_{cd}) and proportion of cruising aircraft (ε) for the three experiments

Experiment	γ_{cd} [^{o}]	ε
Primary	2.8	0.82
Flight-Path Angle	1.4	0.60
	2.8	0.82
	5.6	0.92
Ground Speed	2.8	0.82

Table 6: Aircraft ground speed distributions for the three experiments

Experiment	Distribution	Value [kts]
Primary	Equal	400.0
Flight-Path Angle	Equal	400.0
Ground Speed	Equal	400.0
	Normal	$\mathcal{N}$(400.0, 16.7^2)
	Uniform	$\mathcal{U}$(350.0, 450.0)

at random sector entry-points located on the lower boundary of the 'transition zone'. Subsequently, they climbed to their assigned altitude in the 'cruising zone'. The specific cruising altitude of an aircraft depended on the airspace concept, and can be calculated using equations 27 and 28 for unstructured and layered airspaces, respectively. At a predetermined distance from their destination (which depended on the cruising altitude), aircraft began their descent. As aircraft descended through arbitrary sector exit-points on the lower boundary of the transition zone, they were deleted from the simulation.

It should be noted that all aircraft climbed/descended with equal flight-path angles, see Table 5 for the values used for each experiment. Furthermore, each aircraft maintained a constant ground speed during its flight. The speed distribution of aircraft for the three experiments is listed in Table 6.

5.2.2. Scenario Generation

A scenario generator was created to produce traffic scenarios with a desired and constant traffic density. Constant density scenarios were used so that the number of instantaneous conflicts logged during a simulation run could be attributed to a particular traffic density. Since aircraft were deleted from the simulation as they exited the sector, to realize constant density scenarios, aircraft were introduced into the simulation at a constant spawn rate equal to $\frac{\bar{V}}{\bar{D}}\ N$, where $\bar{V}$ is the average speed of aircraft, $\bar{D}$ is the average trip distance of aircraft, and N is the desired number of instantaneous aircraft. Using this approach, ten traffic demand scenarios of increasing density were defined, ranging between 5-100 aircraft per 10,000 NM^2 in the simulation region. This corresponds to an instantaneous traffic demand of between 80-1600 aircraft in the simulation region; see Table 7. Note that this table displays the number of instantaneous aircraft in both the 'simulation' and 'experiment' regions.

In addition to constant densities, scenarios had a uniform distribution of trip distances and aircraft headings. As explained previously, uniform distance distributions were required to ensure a uniform vertical distribution of traffic.

Table 7: Traffic demand scenarios

#	No. of Inst. AC (Simulation Region)	No. of Inst. AC (Experiment Region)
1	80.0	58.3
2	111.6	81.5
3	155.7	112.2
4	217.2	158.7
5	302.9	218.4
6	422.6	304.9
7	589.4	422.3
8	822.2	588.1
9	1147.0	810.1
10	1600.0	1116.8

Uniform heading distributions were used to maximize the number of instantaneous conflicts [27], thereby making it easier to understand the safety differences between unstructured and layered airspaces.

The horizontal routes for aircraft were selected such that these two requirements were met. This process began by randomly selecting the sector entry-point of an aircraft as any latitude-longitude combination within the simulation region. Subsequently, two uniform random number generators are used to output random values for the heading, ψ_i, and trip distance, D_i, of an aircraft. The sector exit-point of that aircraft is then determined as the end-point of of a straight line with length D_i and a bearing ψ_i from the entry-point. If the corresponding exit-point is outside the simulation region, it is discarded, and the above process is repeated until the entry- and exit-points for all aircraft are inside the simulation region.

It should be noted that all scenarios were generated off-line prior to the simulations. This ensured that all airspace concepts could be subjected to the same traffic demands and horizontal traffic patterns. Additionally, scenarios had a duration of 2 hrs, consisting of a 1 hour traffic volume buildup period, and a 1 hour logging period during which the traffic density was kept constant.

5.3. Independent Variables

Three separate experiments were performed. The independent variables of each experiment are discussed below.

5.3.1. Primary Experiment

The focus of the primary experiment was to validate the conflict count models for under ideal conditions, and to investigate the effect of the allowed heading range per altitude band on the safety of layered concepts. The independent variables of this experiment were:

1. 5 airspace concepts, see Table 3
2. 10 traffic demand scenarios, see Table 7

For each traffic demand scenario, ten repetitions were performed using different traffic realizations (i.e., different initial conditions). This resulted in a total of 500 simulation runs, involving over 950,000 flights.

5.3.2. Flight-Path Angle Experiment

The flight-path angle of climbing and descending traffic, γ_{cd}, is an important parameter that affects the proportion of aircraft in different flight phases, see section 3.2. Hence, an experiment was performed to test conflict count model accuracies for different values of γ_{cd}. The independent variables of this experiment were:

1. 2 airspace concepts, namely UA and L45, see Table 3

2. 10 traffic demand scenarios, see Table 7
3. 3 γ_{cd} settings, see Table 5

Ten repetitions were performed for each traffic demand condition. Therefore, a total of 600 simulations runs were performed for this experiment, using over 1.15 million flights.

5.3.3. Ground Speed Experiment

Since all aircraft were assumed to fly with equal ground speeds by the model derivations, this final experiment considered the sensitivity of the models to this assumption. The independent variables of this experiment were:

1. 2 airspace concepts, namely UA and L45, see Table 3
2. 10 traffic demand scenarios, see Table 7
3. 3 ground speed distributions, see Table 6

As before, ten repetitions were performed for each traffic demand condition, resulting in a total of 600 simulation runs for this experiment, involving over 1.15 million flights.

5.4. Dependent Variables

To determine the accuracy of the conflict count models derived in this paper, model predictions were compared to actual conflict counts logged during the simulations. Model accuracy was quantified by introducing a model accuracy parameter, k, as illustrated below for the basic conflict count model:

$$\text{No. of inst. conflicts} = \underbrace{\text{No. of combinations of two aircraft} \times \text{Conflict probability}}_{\text{Basic conflict count model}} \times k$$

In essence, k is a constant model term that accounts for any factor that was not considered during model derivations. The value of k is determined by fitting the model (right side of above equation) to the conflict count data logged during the simulations (left side of above equation) in a least-square sense. If $k = 1$, then the models, as derived, are able to predict conflict counts with 100% accuracy. On the other hand, if $k < 1$, then model output needs to be scaled down to fit the simulation data, and thus the models are *over-estimating* the measured conflict count. Conversely, if $k > 1$, then model output needs to be scaled up to fit the simulation data, and thus the models are *under-estimating* the measured conflict count.

Since the conflict count model for layered airspaces consists of three terms, see equation 20, three model accuracy parameters are used for layered airspaces, namely, k_{cruise}, $k_{cruise-cd}$ and k_{cd}. These parameters represent model accuracy for conflicts between cruising aircraft, for conflicts between cruising and climbing/descending aircraft, and for conflicts between climbing/descending aircraft, respectively. For UA, only one model accuracy parameter, k_{ua}, is used because no distinctions are made between aircraft in different flight phases by the corresponding conflict count model, see equation 19.

To determine the value of k using least-squares, during the simulations, the number of instantaneous conflicts, and the number of instantaneous aircraft were logged periodically every 15 seconds. Additionally only aircraft within the experiment region, and only conflicts with closest points of approach within the experiment region, were used to assess model accuracy. As mentioned earlier, this method for counting aircraft and conflicts is used because the scenarios used for the simulations had a traffic density of zero near the edges of the simulation region. A similar approach to analyzing simulation data was used in [31].

6. Results

In this section, the results of the three simulation experiments are presented separately. The analysis considers the accuracy of the models, and the intrinsic safety of unstructured and layered airspaces.

6.1. Primary Experiment

As stated previously, the goal of the primary experiment is to measure the accuracy of the conflict count models for both unstructured and layered airspace designs. Additionally, this experiment also investigated the effect of heading range per altitude band on the intrinsic safety of layered concepts. These aspects are considered below.

6.1.1. Validation of Model Structure

Before the absolute accuracy of the models can be evaluated, it is first necessary to examine whether the basic structure of the conflict count models derived in this work, described by equation 1, is sound. In essence, this aspect considers whether the models are able to correctly predict the *shape* of the relationship between the number of instantaneous aircraft and the number of instantaneous conflicts. Based on the structure of equation 1, it can be seen that the ability of the models to correctly describe the shape of the relationship between these two variables is entirely dependent on the *combinatorial* component of the models, which is, by definition, quadratic in nature; see for example equation 16. Therefore, the validity of the structure of the models can be analyzed by fitting simulation logged instantaneous conflict counts, C, to a simple quadratic equation of the form $C = aN^2$, where N is the number of instantaneous aircraft, and a is the quadratic coefficient that relates N to C.

This process is shown in Figure 10 for Unstructured Airspace (UA), and in Figure 11 for Layers 45 (L45). In these figures, the scatter points represent the raw simulation data, while the solid lines represent the least square fit of the aforementioned quadratic curve to the simulation data. Note that the raw data appears in 10 clusters since 10 traffic demand scenarios were used in the simulations, with each cluster representing data collected from all repetitions of a particular demand condition; see Table 7. In addition to the total conflict count, Figure 11 also shows the conflict count results for all flight phase combinations, as required by the model for layered airspaces. Accordingly, the x and y axes of the four graphs in Figure 11 vary according to flight phase; for example, for conflicts between cruising aircraft (top-right), the axes consider the number of instantaneous cruising aircraft and cruising conflicts in the airspace.

From Figures 10 and 11, it can be clearly seen that the number of conflicts does indeed increase quadratically with the number of aircraft in the airspace, confirming the combinatorial component of the models. This conclusion is equally true of the total conflict counts for UA and L45, as it is for the different conflict types of L45. This later result is particularly relevant for layered airspaces, since the corresponding model requires conflicts between aircraft in different flight phases to be treated separately; see equation 20. Because similar trends were found for the other layered airspace concepts, as well as for the flight-path angle and ground speed experiments (not shown), it can be concluded that the overall structure of the models derived in this work is sound.

6.1.2. Model Accuracy

Since this paper proposes *analytical* conflict count models, in addition to checking the overall structure of the models, it is necessary to analyze the absolute accuracy of the models, i.e., the ability of the models to correctly estimate the number of instantaneous conflicts for a given number of instantaneous aircraft and known airspace design parameters (e.g. traffic separation requirements). While validation of the model structure focused on the combinatorial component

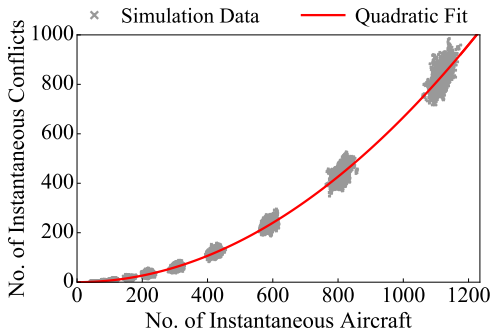

Figure 10: Total conflict count for Unstructured Airspace (UA), primary experiment

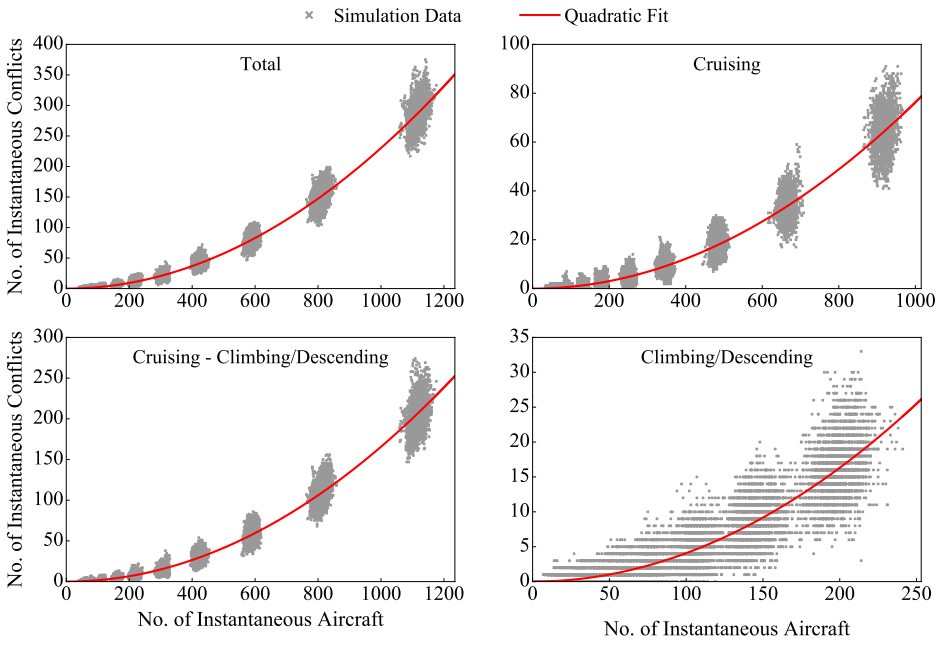

Figure 11: Conflict count per conflict type for Layers 45 (L45), primary experiment

of the models, see section 6.1.1, the absolute accuracy of the models is influenced by both the number of combinations of two aircraft, and the average conflict probability between any two aircraft. Absolute accuracy can be quantified using the model accuracy parameter, k. As described in section 5.4, these 'k-constants' can be thought of as a scaling factor, and thus a value close to 1 indicates high model accuracy, while $k < 1$ and $k > 1$ indicates over- and under-estimation of conflict counts, respectively.

The values of k for the primary experiment are given in Table 8 along with the corresponding percentage accuracy results. Here it can be seen that the overall accuracy of the models is high. For example, for UA (k_{ua}), and for conflicts between cruising aircraft in layered airspaces (k_{cruise}), model accuracy is greater than 90%. However, the table also indicates a consistent over-estimation of conflict counts for interactions involving climbing/descending aircraft, see $k_{cruise-cd}$ and k_{cd} rows of Table 8. This over-estimation is related to the design of the simulation experiments; a more detailed explanation is given with the results of the flight-path angle experiment.

Table 8: Model accuracy, primary experiment

	UA	L360	L180	L90	L45
k_{ua}	1.003 (99.7%)	-	-	-	-
k_{cruise}	-	0.986 (98.6%)	0.977 (97.7%)	0.909 (90.0%)	1.006 (99.4%)
$k_{cruise-cd}$	-	0.884 (86.9%)	0.882 (86.6%)	0.881 (86.5%)	0.867 (84.7%)
k_{cd}	-	0.796 (74.4%)	0.795 (74.1%)	0.791 (73.6%)	0.776 (71.1%)

6.1.3. Effect of Heading Range Per Flight Level on Intrinsic Airspace Safety

In addition to testing the accuracy of the models, data collected during the primary experiment was used to analyze the effect of the allowed heading range per flight level, α, on intrinsic airspace safety; see Figure 12. In this figure, conflicts

are categorized according to the flight phases of interacting aircraft. Furthermore, for each airspace concept, the figure displays the means and the 95% confidence intervals of the number of instantaneous conflicts for all repetitions performed at the highest simulated traffic density. It should be noted that the same trends were observed for all traffic densities (other densities not shown).

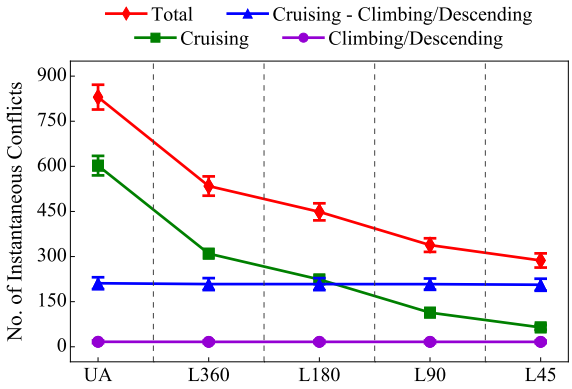

Figure 12: Means and 95% confidence intervals of the conflict count per conflict type at the highest traffic density, primary experiment

Figure 12 shows that a decrease of α from L360 to L45 lowers the *total* conflict count (red line). Additionally, it can be seen that this safety improvement is entirely due to the reduction of conflicts between cruising aircraft when α is decreased (green line). Because all layered concepts used the same number of flight levels, based on the conflict count model for cruising aircraft in layered airspaces, given by equation 24, this increased safety can be explained by the reduction of horizontal relative velocities when α is decreased.

Interestingly, Figure 12 also shows that the number of conflicts involving climbing and descending traffic is invariant with α (blue and violet lines). This is because none of the airspace concepts considered here apply any constraints on the paths of climbing and descending traffic. While the absolute number of conflicts with climbing/descending aircraft remains constant, the proportion of such conflicts increases as α is decreased. This can be seen clearly for the L45 concept, for which 77.8% of the total conflicts is caused by climbing/descending traffic. This suggests that climbing/descending aircraft have a greater influence on the overall intrinsic safety of layered concepts with a narrow heading range per flight level.

Since α only affects the number of cruising conflicts, the corresponding conflict model for cruising aircraft, see equation 24, can be used to predict the beneficial effect of reducing α on the intrinsic safety of layered concepts; see Table 9. Note that this table shows the percentage reduction of conflicts relative to the case with the highest horizontal relative velocities, i.e, relative to $\alpha = 360^o$. Here it can be seen that linearly decreasing α results in a non-linear decrease in the number of conflicts. Furthermore, this table also shows that the model predicted reductions are closely matched by the simulation logged conflict reductions. This once again demonstrates the high accuracy of the models, and also illustrates how the models can be used to understand the effects of other airspace design parameters, such as separation requirements, on intrinsic safety.

Table 9: Effect of heading range per flight level on predicted and actual conflict count reductions

Heading Range Per Layer, α	Model Prediction	Simulation Results
360^o	0%	0%
180^o	27.3%	27.9%
90^o	60.1%	63.3%
45^o	79.6%	79.2%

Although the analysis thus far has focused on layered airspaces, Figure 12 can also be used to compare the safety of

UA with that of layered concepts. In relation to this aspect, Figure 12 shows that UA results in significantly more (total) conflicts than for any of the layered concepts. This is also true when comparing UA to the L360 concept. Since there are no heading-altitude constraints, and therefore no reductions in relative velocities, for either of these two concepts, the increased safety of L360 can be attributed to the only other difference between UA and layered concepts, i.e., the use of predefined flight levels for cruising aircraft in layered concepts. As a result of these predefined flight levels, the model for layered airspaces predicts a 30.9% reduction of the total conflicts for L360 when compared to UA at the highest traffic demand (this matches well to the 35.5% reduction logged during the simulations).

6.2. Flight-Path Angle Experiment

For a given set of origins, destinations and cruising altitudes, the flight path angle of climbing and descending traffic, γ_{cd}, affects the ratio between the number of instantaneous of cruising vs. climbing/descending aircraft. This is because a higher value of γ_{cd} causes an aircraft to climb faster to its cruising altitude, leading to a higher proportion of cruising aircraft. Since the proportion of aircraft in different flight phases influences both the expected vertical relative velocity and the average conflict probability between aircraft, the effect of γ_{cd} on the intrinsic safety of the UA and L45 concepts has been analyzed in this experiment. To this end, simulations were repeated for $\gamma_{cd} = \{1.4^o, 2.8^o, 5.6^o\}$.

6.2.1. Effect of Flight-Path Angle on Intrinsic Airspace Safety

Total conflict count results for the flight-path angle experiment are displayed in Figure 13. For UA, Figure 13(a) shows that an increase of γ_{cd} increases the number of conflicts between cruising aircraft (green line). This trend is expected since the number of cruising aircraft increases with γ_{cd}. Additionally, an increase of γ_{cd} reduces the proportion of climbing/descending aircraft, leading to a corresponding decrease of such conflicts (blue and violet lines). Because these two effects are (nearly) equal, but opposite in magnitude, changes to γ_{cd} only have a minor effect on the total conflict count for UA (red line).

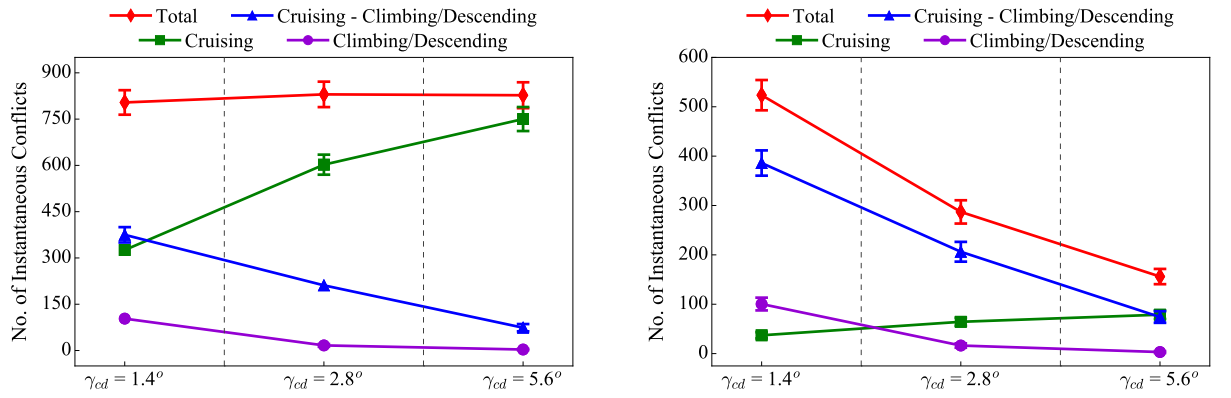

(a) Unstructured Airspace (UA) **(b) Layers 45 (L45)**

Figure 13: Means and 95% confidence intervals of the conflict count per conflict type for Unstructured Airspace and Layers 45 at the highest traffic density, flight-path angle experiment

In contrast, Figure 13(b) shows that γ_{cd} has a substantial effect on the total conflict count for L45 (red line) , with safety increasing for higher γ_{cd}. Although the number of conflicts involving cruising aircraft increases for L45 (green line), it does so at a lower pace than for UA. In fact, the total conflict count for L45 is mainly influenced by conflicts between cruising and climbing/descending aircraft (blue line). This matches the trend found for the primary experiment, where the majority of conflicts for layered airspaces with a narrow heading range per flight level involve climbing/descending aircraft.

6.2.2. Effect of Flight-Path Angle on Model Accuracy

The effect of γ_{cd} on model accuracy is displayed in Table 10. As exemplified by the total conflict count in Figure 13, Table 10 shows only a minor effect of γ_{cd} on model accuracy for UA, and for conflicts between cruising aircraft in

layered airspaces (see k_{ua} and k_{cruise} rows). However, accuracy for conflicts involving climbing/descending aircraft in layered airspaces appears to be significantly affected by γ_{cd}. As noted for the results of the primary experiment, the models show a tendency to over-estimate the number of such conflicts. Furthermore, the degree of this overestimation worsens as γ_{cd} increases.

Table 10: Model accuracy, flight-path angle experiment

		$\gamma_{cd} = 1.4^o$	$\gamma_{cd} = 2.8^o$	$\gamma_{cd} = 5.6^o$
UA	k_{ua}	0.973 (97.2%)	1.003 (99.7%)	1.003 (99.7%)
L45	k_{cruise}	1.081 (92.5%)	1.006 (99.4%)	0.991 (99.1%)
	$k_{cruise-cd}$	1.030 (97.1%)	0.867 (84.7%)	0.589 (30.1%)
	k_{cd}	0.916 (90.9%)	0.776 (71.1%)	0.681 (53.2%)

An explanation for this trend can be found by considering the design of the simulation experiments, and the relationship between γ_{cd} and the volume of airspace searched for conflicts during conflict detection. Since γ_{cd} affects the magnitude of the vertical relative velocity, it also affects the size of the *vertical volume* of airspace searched for conflicts by aircraft; see Figure 6(b). Furthermore, no traffic was simulated above and below the 'simulation' and 'experiment' regions; see Figure 9. Therefore, climbing/descending aircraft, with vertical conflict search volumes that extend outside the simulated sector, are less likely to detect conflicts when compared to similar aircraft in the middle altitudes of the simulation. Because an increase in γ_{cd} increases the size of the vertical conflict search volume, the number of climbing/descending aircraft that are negatively affected by this effect increases with γ_{cd}, leading to a greater over-estimation by the conflict count models.

It should be noted that, unlike the vertical direction, the model accuracy results for cruising conflicts is *not* affected by the fact that no traffic was simulated outside the simulated sector. Although cruising conflict counts are affected by the *horizontal volume* of airspace searched for conflicts in UA, and the *horizontal area* of airspace in layered concepts, only conflicts with closest points of approach within the 'experiment' region were considered for model accuracy analysis, as explained in section 5.4. Therefore, even if the horizontal conflict search volume/area extends beyond the 'experiment region', the gap between the 'experiment' and 'simulation' regions; see Figure 9, compensates for this unrealistic aspect of the simulation's design.

However, a similar distinction between 'experiment' and 'simulation' regions is not feasible in the vertical direction since data from all cruising flight levels is needed to evaluate model accuracies for layered airspaces. Moreover, a sudden drop in densities is more realistic in the vertical direction; for example, commercial aircraft do not usually fly above 45,000 ft. On the other hand, changes in traffic density tend to be less abrupt in the horizontal direction for real operations (except near and over oceans), thus justifying the distinction between experiment and simulation regions used here in the horizontal plane.

6.3. Ground Speed Experiment

The analytical conflict count models derived in this paper assume equal ground speeds for all aircraft. This assumption was required to simplify a complex expression that is used to compute the expected horizontal relative velocity between aircraft, see equation 4. However, this assumption is not representative of current day en route operations because optimum cruising speeds vary with aircraft type, and because wind direction and speed, which affects ground speed calculation, can vary significantly over large areas of airspace. Additionally, the equal ground speed assumption does not allow for the possibility of overtaking conflicts between aircraft. Consequently, to assess the sensitivity of the models to the equal ground speed assumption, simulations were repeated for cases where the grounds speeds of aircraft were normally and uniformly distributed for the UA and L45 concepts.

6.3.1. *Effect of Ground Speed Distribution on Intrinsic Airspace Safety*

Figure 14 shows that speed distribution has a negligible effect on conflict counts for UA. This is also largely true for L45, except for the slight increase in conflicts between cruising aircraft when the speed distribution changes from 'equal' to 'uniform' (green line). This invariance of conflict counts with speed distribution can be explained by the fact that the same average ground speed is used by all three distributions (to enable a fair comparison). Therefore, while the speed distribution of aircraft may have an effect at a per aircraft level, the overall intrinsic safety provided unstructured and layered airspaces is largely unaffected by the shape of the ground speed distribution, and is only dependent on the magnitude of the average speed of all aircraft in the airspace.

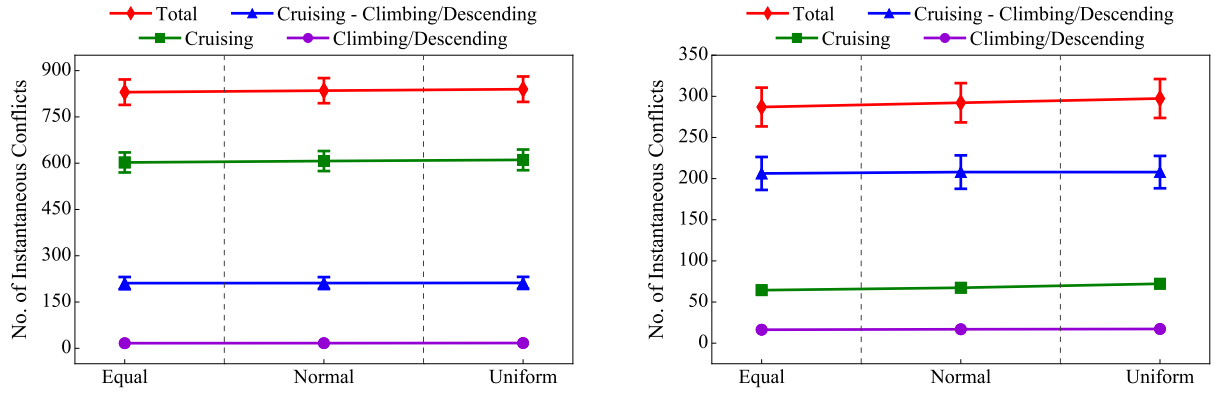

(a) Unstructured Airspace (UA) **(b) Layers 45 (L45)**

Figure 14: Means and 95% confidence intervals of the conflict count per conflict type for Unstructured Airspace and Layers 45 at the highest traffic density, ground speed experiment

6.3.2. *Effect of Ground Speed Distribution on Model Accuracy*

The model accuracy results for the ground speed experiment are displayed in Table 11. Here it should be noted that the model was evaluated assuming equal ground speeds for all aircraft, regardless of the actual ground speed distributions used in the simulations. The table shows that model accuracy for UA is not dependent on ground speed distribution. Similarly, for L45, model accuracy for conflicts involving climbing and descending aircraft is not significantly different to the condition with equal ground speeds. On the other hand, accuracy for conflicts between cruising aircraft decreases with increasing variation in aircraft ground speeds for L45. This suggests that restricting the heading range per altitude level negatively affects the accuracy of the models for layered concepts.

Table 11: Model accuracy, ground speed experiment

		Equal	Normal	Uniform
UA	k_{ua}	1.003 (99.7%)	1.006 (99.4%)	1.006 (99.4%)
L45	k_{cruise}	1.006 (99.4%)	1.053 (95.0%)	1.118 (89.4%)
	$k_{cruise-cd}$	0.867 (84.7%)	0.873 (85.4%)	0.866 (84.5%)
	k_{cd}	0.776 (71.1%)	0.799 (74.8%)	0.809 (76.4%)

As mentioned above, the equal ground speed assumption affects the calculation of the expected horizontal relative velocity between aircraft, $\mathbf{E}(v_{r,h})$. To gain a better sense on the effect of this assumption on $\mathbf{E}(v_{r,h})$, equation 4 is evaluated numerically for all three speed distributions for the UA and L45 concepts, see Table 12. This table shows that changing the speed distribution has a much greater effect on $\mathbf{E}(v_{r,h})$ for L45; a 10.3% increase occurs when the speed

distribution is changed from 'equal' to 'uniform' for L45, while a similar change of speed distribution only results in a 0.5% increase for UA. Since $\mathbf{E}(v_{r,h})$ directly affects the conflict count model for cruising aircraft in layered airspaces, the trends shown in Table 12 explain the model accuracy results noted above for this experiment.

Table 12: Numerically computed values of the expected horizontal relative velocities for Unstructured Airspace (UA) and Layers 45 (L45)

	Equal	Normal	Uniform
UA [kts]	509.30	507.42	511.66
L45 [kts]	103.92	107.46	114.66

Table 13: Effect of analytical and numerical methods of estimating the expected horizontal relative velocity on model accuracy for Layers 45

	Equal	Normal	Uniform
k_{cruise} Analytical	1.006 (99.4%)	1.053 (95.0%)	1.118 (89.4%)
k_{cruise} Numerical	1.006 (99.4%)	1.018 (98.2%)	1.013 (98.7%)

Although this work focuses on developing fully *analytical* models, the *numerical* $\mathbf{E}(v_{r,h})$ values listed in Table 12 can be used to increase model accuracy for cruising conflicts in layered concepts. To this end, Table 13 displays accuracy results for k_{cruise} for analytically and numerically computed $\mathbf{E}(v_{r,h})$ for L45. Here it can be seen that accuracy for the normal and the uniform speed distributions increases to the level reported for the equal speed case when numerical values of $\mathbf{E}(v_{r,h})$ are used. But for UA, as well as for conflicts involving climbing/descending aircraft in L45, using numerical values of $\mathbf{E}(v_{r,h})$ does not significantly affect model accuracy (not shown). Therefore, based on the results shown in Figure 14, it can be concluded that the analytical models derived using the equal speed assumption can be used to understand and explain the factors that affect the intrinsic safety of unstructured and layered airspaces.

7. Discussion

In this paper, analytical conflict count models were developed to analyze the intrinsic safety of unstructured and layered airspace designs. The models focused on quantifying the effect of airspace design parameters and traffic demand on the number of instantaneous system-wide conflicts. The models were validated using extensive fast-time simulation experiments that involved over three million flights. This section reflects on the intrinsic safety offered by unstructured and layered airspaces, and discusses the accuracy of the models. Additionally, important aspects related to model usage are also considered.

7.1. Intrinsic Safety of Unstructured and Layered Airspace Designs

The results of all simulation experiments performed in this study showed that aircraft in unstructured airspace are subject to more conflicts than aircraft in layered airspaces. The higher intrinsic safety of layered airspaces can be attributed to two factors that reduce the number of conflicts between cruising aircraft.

The first factor is related to the allowed heading range per flight level. For layered concepts that reduce the allowed heading range per flight level, relative velocities between cruising aircraft are reduced compared to unstructured airspace. This reduction in relative velocities, which stems from a greater alignment of cruising traffic in each flight level, reduces conflict probabilities between neighboring aircraft. While this effect was already hypothesized in our prior work [14], the current study quantifies this effect, and shows that the corresponding safety benefits are nonlinear with the allowed heading range. For example, lowering the heading range per flight level from 360^o to 90^o reduces the number of conflicts between cruising aircraft by approximately 60%. However, further halving the heading range per flight level to 45^o only provides an additional 20% reduction in conflicts.

The second factor that improves the safety performance of layered airspaces is the use of predefined flight levels for cruising aircraft. Using predefined flight levels not only reduces the number of combinations of aircraft that can conflict with each other, it also reduces the conflict probability between aircraft. This is because in layered airspaces, conflicts can only occur between cruising aircraft if both aircraft are at the same flight level. Consequently, in layered concepts, conflict probability for cruising aircraft is a function of the *area* searched for conflicts. On the other hand, conflict probability is directly proportional to the *volume* searched for conflicts in unstructured airspace, since there are

no vertical constraints on aircraft motion. The larger region of airspace searched for conflicts in unstructured airspace, therefore, increases conflict probability and the number of conflicts encountered by cruising aircraft.

Although layered designs improve the overall safety of en route airspaces by reducing conflicts between cruising aircraft, it is worth noting that no differences were observed between unstructured and layered concepts in relation to the number of conflicts involving climbing/descending aircraft. In fact, the simulation results clearly showed that as the heading range per flight level is decreased, the *proportion* of conflicts involving climbing/descending aircraft is increased. Therefore, such conflicts can become more influential than conflicts between cruising aircraft, particularly for layered airspaces with a narrow heading range per flight level. While the magnitude of this trend is affected by the ratio of cruising vs. climbing/descending aircraft, which is in turn influenced by the flight path angles of climbing and descending traffic, this result does emphasize the need to take into account conflicts between aircraft in different phases when assessing the overall intrinsic safety of an airspace design.

7.2. Conflict Count Model Validation

By comparing simulation results to model predictions, model accuracy was determined to be high for both airspace designs. For example, in addition to correctly predicting the shape of the relationship between the numbers of instantaneous aircrafts and conflicts, the models could also estimate the effect of the allowed heading range per flight level on conflict counts with an accuracy greater than 90% the models could also calculate the effect of using predefined cruising altitudes on safety with a similar level of accuracy.

The accuracy of all models is, to some degree, affected by the assumptions upon which they are derived. The models derived here are no exception to this rule, and two assumptions negatively affected conflict count estimation. The first assumption was that all aircraft have equal ground speeds, and it was required to derive purely *analytical* conflict count models. Because this assumption does not consider the occurrence of over-taking conflicts, and because such conflicts are more likely to occur as the heading range per altitude band is decreased, model accuracy for layered airspaces was negatively affected by this assumption. Nevertheless, accuracy was shown to be increased to the level found for the equal speed assumption when the analytical models were augmented with numerically computed values of the expected horizontal relative velocity. It is hypothesized that the effect of other traffic scenario related assumptions, such as the uniformly distributed heading distributions used in this work, can also be compensated for in a similar manner. Such changes could be used to expand the models to account for the traffic flow and demand distributions of current-day operations.

Model accuracy was also affected by the fact that the models assume airspace to be infinite in extent, both horizontally and vertically. While this assumption is convenient for modeling purposes, it is an obvious deviation from reality. Therefore, the simulations performed to validate the models used a finite volume of airspace. Although this approach made the simulations more realistic, it also caused traffic density to drop to zero at the boundaries to the simulated sector. Since traffic density rarely drops so drastically in the horizontal direction for real operations, the models were only validated for data logged within a horizontally defined experiment region at the center of the simulated sector. However, a similar approach in the vertical direction was deemed to be unrealistic, given the altitude related flight envelope limitations of aircraft. Therefore, the accuracy results presented in this paper are representative of the range of values that could be obtained using the models for real operations, if such data were to become available in the future for unstructured and layered en route airspaces.

Despite these limitations, as noted above, model accuracy was generally quite high. This high accuracy allows the models to be used as tools to compare unstructured and layered airspaces, as well as to evaluate the effects of a number of safety relevant parameters, such as conflict detection look-ahead time and traffic separation requirements. Additionally, since the models derived here take into account the proportion of aircraft in different flight phases when computing conflict counts, they provide a more comprehensive understanding on the overall intrinsic safety provided by a particular airspace design when compared to previous studies that have only considered cruising aircraft. This aspect is particularly important during the design of layered airspaces where, as noted above, climbing/descending traffic can cause the majority of conflicts under certain design choices.

7.3. Additional Considerations

Although the models were tested within the context of high-altitude commercial operations, they can also be applied to the design and analysis of unstructured and layered airspace concepts for low-altitude unmanned aircraft ops. This is possible because the generic, analytical nature of the models allows a generalization of the results beyond the specific conditions that have been simulated in this study, for instance for the lower speeds anticipated for unmanned traffic. On a similar note, the underlying approach used here to model system-wide conflict counts could, with some additions, also be expanded to other airspace designs, including for concepts closer to today's mode of operations. Any adaptations along these lines would require an analysis of how the constraints imposed by a particular airspace design affect the number of combinations of two aircraft, and the average (horizontal and vertical) relative velocities between aircraft.

It is important to realize that the conflict count models considered here measure safety as a function of airspace design *only*. Other factors that affect safety, including uncertainties related to aircraft state measurement/communication, are not considered by the models since these aspects are not directly affected by the design of an airspace. Nevertheless, a recent study has concluded that the characteristics of the Automatic Dependent Surveillance-Broadcast (ADS-B) system, which is the system that is promoted by many ATM organizations to supplement, and eventually replace, radar-based surveillance, has little effect on the performance of the state-based conflict detection method used here [37]. Therefore, uncertainties related to aircraft state measurement/communication are not expected to significantly affect the results presented here, particularly for future operations with ADS-B.

Another factor that is not considered by the notion of *intrinsic safety*, and by the models presented here, is the effect of tactical conflict resolutions on airspace safety. In fact, the *overall safety* of operations is affected by both the selected airspace design and the selected conflict resolution approach. This is particularly the case at high traffic densities because the scarcity of airspace could trigger conflict chain reactions when conflict resolution actions are taken. For a more detailed analysis on the effect of conflict chain reactions on safety, the reader is referred to [15].

Many ATM studies interrelate airspace safety and capacity. Although these two metrics are closely connected, airspace concepts that maximize safety need not be the optimum in terms of other relevant performance metrics, most notably airspace efficiency. The balance between safety and efficiency should be an important consideration when arguing for or against a particular airspace design, or when fine-tuning the parameters of the selected airspace design. This notion can be illustrated for the layers concept; although decreasing the heading range per flight level improves safety, it also increases the number of flight levels needed to specify all possible travel directions. Therefore, for a given volume of airspace, it may be more efficient to use a value for the heading range per flight level that allows multiple complete layer sets to be defined, since this approach could minimize the fuel penalty of using predefined cruising altitudes in layered airspaces. To summarize, when evaluating the *capacity* of an airspace design, it is necessary to consider the effect of a design on multiple airspace performance metrics in unison, including safety and efficiency. The approach used to model intrinsic airspace safety in this paper is a good starting point to develop a capacity assessment method along these lines.

8. Conclusions

This paper presented analytical conflict count models to measure the intrinsic safety of unstructured and layered en-route airspace designs. The models take into account the three-dimensional motion of aircraft, and therefore improve upon previous studies by considering conflicts between aircraft in different flight phases. Fast-time simulation experiments were performed to validate the models, and compare unstructured and layered airspaces in terms of the intrinsic safety they provide. The following conclusions can be drawn:

1. *Layered airspace concepts were found to be safer than unstructured airspace.* This is because layered airspaces restrict the heading range allowed per flight level, and because they use predefined flight levels to reduce the number of possible conflict pairs.
2. *The safety performance of layered airspaces increases as the heading range per flight level is reduced.* This can be explained by the reduction of relative velocities between cruising aircraft as the heading range per flight level is decreased. The relationship between the number of instantaneous conflicts and the heading range per flight level is nonlinear.

3. *The safety benefits of layered airspaces only apply to cruising aircraft*, and no differences were found between unstructured and layered airspaces with respect to the number of conflicts involving climbing/descending aircraft. For this reason, the safety of layered airspaces is more sensitive to the proportion of cruising aircraft. This result also emphasizes the need to consider aircraft in different flight phases when evaluating the overall safety of an airspace design.
4. *The 3D analytical conflict count models derived here were able to estimate conflict counts for both unstructured and layered concepts with high accuracy*, and were able to predict the aforementioned benefits of layered airspaces. Consequently, they can be used to understand the relationships between the parameters that affect safety for both these airspace concepts, including the effect of the proportion of aircraft in different flight phases on instantaneous conflict counts.
5. *Augmenting the analytical models with numerically computed values of the expected relative velocity between aircraft was shown to further increase model accuracy.* This approach can be used to take into account the effects of other traffic demand and flow conditions that have not been considered in this study.

Acknowledgments

The authors would like to thank Ólafur Þórðarson (MSc student TU Delft) for his assistance in numerically computing the expected relative velocity. Needless to add, this research would not have been possible without the efforts of the open-source community that continually contributes to the development of the BlueSky ATM simulator. This research did not receive any specific grant from funding agencies in the public, commercial, or not-for-profit sectors.

References

[1] N. A. Doble, R. Hoffman, P. U. Lee, J. Mercer, B. Gore, N. Smith, K. Lee, Current airspace configuration practices and their implications for future airspace concepts, in: AIAA Aviation Technology, Integration and Operations (ATIO) Conference, AIAA-2008-8936, Anchorage, 2008. doi:10.2514/6.2008-8936.
URL http://arc.aiaa.org/doi/pdf/10.2514/6.2008-8936

[2] Magill, S. A. N., Effect of Direct Routing on ATC Capacity, in: USA/Europe Air Traffic Management R&D Seminar, Orlando, 1998.
URL http://www.atmseminar.org/seminarContent/seminar2/papers/p_022_APMMA.pdf

[3] P. Dell'Olmo, G. Lulli, A new hierarchical architecture for Air Traffic Management: Optimisation of airway capacity in a Free Flight scenario, European Journal of Operational Research 144 (1) (2003) 179–193. doi:10.1016/S0377-2217(01)00394-0.
URL http://www.sciencedirect.com/science/article/pii/S0377221701003940

[4] Performance Review Commission, Eurocontrol Performance Review Report 2016, Tech. Rep. PRR2016, Eurocontrol (2016).
URL http://www.eurocontrol.int/news/performance-review-report-2016

[5] J. J. Rebollo, H. Balakrishnan, Characterization and prediction of air traffic delays, Transportation Research Part C: Emerging Technologies 44 (Supplement C) (2014) 231–241. doi:10.1016/j.trc.2014.04.007.
URL http://www.sciencedirect.com/science/article/pii/S0968090X14001041

[6] SESAR Consortium, The Concept of Operations at a glance, Tech. rep., Single European Sky (2007).

[7] Joint Planning and Development Office, Concept of operations for the Next Generation Air Transportation System, Tech. rep., FAA (Jun. 2007).

[8] J. M. Hoekstra, R. N. H. W. van Gent, R. C. J. Ruigrok, Designing for safety: the 'free flight' air traffic management concept, Reliability Engineering & System Safety 75 (2) (2002) 215–232. doi:10.1016/S0951-8320(01)00096-5.
URL http://www.sciencedirect.com/science/article/pii/S0951832001000965

[9] S. M. Green, K. D. Bilimoria, M. G. Ballin, Distributed air/ground traffic management for en route flight operations, Air Traffic Control Quarterly 9 (4) (2001) 259–285.
URL https://arc.aiaa.org/doi/abs/10.2514/atcq.9.4.259

[10] K. Bilimoria, K. Sheth, H. Lee, S. Grabbe, Performance evaluation of airborne separation assurance for free flight, in: AIAA Guidance, Navigation and Control Conference, AIAA-2000-4269, 2000. doi:10.2514/6.2000-4269.
URL http://arc.aiaa.org/doi/abs/10.2514/6.2000-4269

[11] J. Krozel, M. Peters, K. Bilimoria, C. Lee, J. Mitchell, System performance characterisitcs of centralized and decentralized air traffic separation strategies, in: USA/Europe Air Traffic Management R&D Seminar, 2001.

[12] A. Barnett, Free-Flight and en Route Air Safety: A First-Order Analysis, Operations Research 48 (6) (2000) 833–845. doi:10.1287/opre.48.6.833.12394.
URL http://pubsonline.informs.org/doi/citedby/10.1287/opre.48.6.833.12394

[13] NMD/NSD Operations Roadmap Team, European Free Route Airspace Developments, Tech. rep., Eurocontrol (2015).

[14] E. Sunil, J. Ellerbroek, J. Hoekstra, A. Vidosavljevic, M. Arntzen, F. Bussink, D. Nieuwenhuisen, Analysis of Airspace Structure and Capacity for Decentralized Separation Using Fast-Time Simulations, Journal of Guidance, Control, and Dynamics 40 (1) (2017) 38–51. doi:10.2514/1.G000528.
URL http://dx.doi.org/10.2514/1.G000528

[15] M. R. Jardin, Analytical Relationships Between Conflict Counts and Air-Traffic Density, Journal of Guidance, Control, and Dynamics 28 (6) (2005) 1150–1156. doi:10.2514/1.12758.
URL http://dx.doi.org/10.2514/1.12758

[16] R. Irvine, H. Hering, Towards Systematic Air Traffic Management in a Regular Lattice, in: 7th AIAA ATIO Conf, 2nd CEIAT Int'l Conf on Innov and Integr in Aero Sciences, 17th LTA Systems Tech Conf; followed by 2nd TEOS Forum, 2007, p. 7780.
URL http://arc.aiaa.org/doi/pdf/10.2514/6.2007-7780

[17] K. Leiden, S. Peters, S. Quesada, Flight level-based dynamic airspace configuration, in: Proceedings of the 9th AIAA Aviation Technology, Integration and Operations (ATIO) Forum. American Institute of Aeronautics and Astronautics, 2009.
URL http://arc.aiaa.org/doi/pdf/10.2514/6.2009-7104

[18] R. A. Paielli, A Linear Altitude Rule for Safer and More Efficient Enroute Air Traffic, Air Traffic Control Quarterly 8 (3).
URL http://www.aviationsystemsdivision.arc.nasa.gov/publications/2000/Paielli_ATCQ_Alt-Rules_2000.pdf

[19] International Civil Aviation Organization, Annex 2, Rules of the Air, Tech. rep. (Jul. 2005).

[20] Norman Davidson, Statistical Mechanics, Dover Publications, 2003.

[21] B. L. Marks, Air Traffic Control Separation Standards and Collision Risk, Tech. Rep. MATH 91 (1963).
URL https://trid.trb.org/view.aspx?id=618712

[22] P. G. Reich, Analysis of Long-Range Air Traffic Systems: Separation Standards—I, The Journal of Navigation 19 (01) (1966) 88–98. doi:10.1017/S037346330004056X.

[23] P. G. Reich, Analysis of Long-Range Air Traffic Systems: Separation Standards—III, The Journal of Navigation 19 (3) (1966) 331–347. doi:10.1017/S0373463300047445.
URL https://www.cambridge.org/core/journals/journal-of-navigation/article/analysis-of-longrange-air-traffic-systems-separation-standardsiii/F66DD3220162FC9B49774AA13DC0ED07

[24] P. Brooker, Future Air Traffic Management: Quantitative En Route Safety Assessment Part 2 – New Approaches, The Journal of Navigation 55 (3) (2002) 363–379. doi:10.1017/S037346330200187X.

[25] F. Netjasov, Framework for airspace planning and design based on conflict risk assessment: Part 1: Conflict risk assessment model for airspace strategic planning, Transportation Research Part C: Emerging Technologies 24 (2012) 190–212. doi:10.1016/j.trc.2012.03.002.
URL http://www.sciencedirect.com/science/article/pii/S0968090X12000435

[26] F. Netjasov, O. Babić, Framework for airspace planning and design based on conflict risk assessment: Part 3: Conflict risk assessment model for airspace operational and current day planning, Transportation Research Part C: Emerging Technologies 32 (2013) 31–47. doi:10.1016/j.trc.2013.04.002.
URL http://www.sciencedirect.com/science/article/pii/S0968090X13000752

[27] S. Endoh, Aircraft collision models, Ph.D. thesis, Massachusetts Institute of Technology, Flight Transportation Laboratory (1982).
URL http://dspace.mit.edu/handle/1721.1/68072

[28] W. Graham, R. H. Orr, Terminal Air Traffic Model with Near Midair Collision and Midair Collision Comparison, Tech. rep., US Department of Transportation-Air Traffic Control Advisory Committee (1969).

[29] P. D. Flanagan, K. E. Willis, Frequency of airspace conflicts in the mixed terminal environment, Tech. rep., US Department of Transportation - Air Traffic Control Advisory Committee (1969).

[30] K. Datta, R. M. Oliver, Predicting risk of near midair collisions in controlled airspace, Transportation Research Part B: Methodological 25 (4) (1991) 237–252. doi:10.1016/0191-2615(91)90006-5.
URL http://www.sciencedirect.com/science/article/pii/0191261591900065

[31] S. Ratcliffe, R. L. Ford, Conflicts between Random Flights in a Given Area, The Journal of Navigation 35 (01) (1982) 47–74. doi:10.1017/S0373463300043101.
URL http://journals.cambridge.org/article_S0373463300043101

[32] R. L. Ford, On the Use of Height Rules in Off-route Airspace, The Journal of Navigation 36 (02) (1983) 269–287. doi:10.1017/S037346330002498X.
URL http://journals.cambridge.org/article_S037346330002498X

[33] Hoekstra, J., Maas, J., Tra, M., Sunil, E., How Do Layered Airspace Design Parameters Affect Airspace Capacity and Safety?, in: Proceedings of the 7th International Conference on Research in Air Transportation, 2016.

[34] Dimitrios Milios, Probability Distributions as Program Variables, Master's thesis, University of Edinburgh (2009).
URL http://www.inf.ed.ac.uk/publications/thesis/online/IM090722.pdf

[35] J. Hoekstra, J. Ellerbroek, BlueSky ATC Simulator Project: an Open Data and Open Source Approach, in: Proceedings of the 7th International Conference on Research in Air Transportation, 2016.

[36] I. Metz, J. Hoekstra, J. Ellerbroek, D. Kugler, Aircraft Performance for Open Air Traffic Simulations, in: AIAA Modeling and Simulation Technologies Conference, 2016.

[37] T. Langejan, E. Sunil, J. Ellerbroek, J. Hoekstra, Effect of ADS-B Characteristics on Airborne Conflict Detection and Resolution, in: Proccedings of the 6th Sesar Innovation Days, 2016.